SCIENTIFIC REPORTS

OPEN

SUBJECT AREAS:
DRUG DEVELOPMENT
NATURAL PRODUCTS

Received
2 September 2014

Accepted
5 January 2015

Published
28 January 2015

Resveratrol Prevents Age-Related Memory and Mood Dysfunction with Increased Hippocampal Neurogenesis and Microvasculature, and Reduced Glial Activation

Maheedhar Kodali[1,2,3*], Vipan K. Parihar[4*†], Bharathi Hattiangady[1,2,3,4], Vikas Mishra[1,2,3], Bing Shuai[1,2,3,4] & Ashok K. Shetty[1,2,3,4]

[1]Institute for Regenerative Medicine, Texas A&M Health Science Center College of Medicine at Scott & White, Temple, Texas, USA, [2]Research Service, Olin E. Teague Veterans Affairs Medical Center, Central Texas Veterans Health Care System, Temple, Texas, USA, [3]Department of Molecular and Cellular Medicine, Texas A&M Health Science Center College of Medicine, College Station, Texas, USA, [4]Department of Surgery (Neurosurgery) and Research Service, Duke University and Veterans' Affairs Medical Centers, Durham, North Carolina, USA.

Correspondence and requests for materials should be addressed to A.K.S. (Shetty@medicine.tamhsc.edu)

* These authors contributed equally to this work.

† Current address: Department of Radiation Oncology, Univ California Irvine.

Greatly waned neurogenesis, diminished microvasculature, astrocyte hypertrophy and activated microglia are among the most conspicuous structural changes in the aged hippocampus. Because these alterations can contribute to age-related memory and mood impairments, strategies efficacious for mitigating these changes may preserve cognitive and mood function in old age. Resveratrol, a phytoalexin found in the skin of red grapes having angiogenic and antiinflammatory properties, appears ideal for easing these age-related changes. Hence, we examined the efficacy of resveratrol for counteracting age-related memory and mood impairments and the associated detrimental changes in the hippocampus. Two groups of male F344 rats in late middle-age having similar learning and memory abilities were chosen and treated with resveratrol or vehicle for four weeks. Analyses at ~25 months of age uncovered improved learning, memory and mood function in resveratrol-treated animals but impairments in vehicle-treated animals. Resveratrol-treated animals also displayed increased net neurogenesis and microvasculature, and diminished astrocyte hypertrophy and microglial activation in the hippocampus. These results provide novel evidence that resveratrol treatment in late middle age is efficacious for improving memory and mood function in old age. Modulation of the hippocampus plasticity and suppression of chronic low-level inflammation appear to underlie the functional benefits mediated by resveratrol.

The hippocampus, a region of the brain vital for functions such as learning, memory and mood, is highly vulnerable to normal aging and Alzheimer's disease (AD)[1]. Because the pathogenesis leading to AD includes an extended latent phase and a shorter prodromal, mild cognitive impairment (MCI) phase[2], drug interventions that can prevent MCI in old age have immense importance. Such drugs may be prescribed to the aging population if they are efficacious for maintaining normal cognitive and mood function in old age with no or minimal side effects. Decreased function in the dentate gyrus (DG) of the hippocampus has been considered as one of the key reasons for memory and mood dysfunction seen in old age[3,4]. The DG exhibits a unique form of neural circuit plasticity all through life called "adult hippocampus neurogenesis"[5–7]. Interestingly, neurons that are born in the adult DG play important roles in memory and mood function[6,8–10]. Because aging is associated with greatly diminished hippocampal neurogenesis[11–13], the proposition that declined neurogenesis contributes to memory and mood dysfunction in the aged population has emerged. This concept has been supported by multiple studies[14]. These include observations that middle-aged/aged animals housed in enriched environment, performing voluntary physical exercise or exhibiting lower corticosterone levels display improved cognitive function in association with enhanced hippocampus neurogenesis[15–18]. Furthermore, progenitor cells in the hippocampus of depressed patients exhibit decreased proliferation than age-matched controls[19].

Studies in rat models suggest that aging does not diminish the numbers of putative hippocampal neural stem/progenitor cells (NSCs) or impair the neuronal differentiation and survival of newly born cells[12,13,20]. However, the fraction of quiescent NSCs increases in the aged hippocampus[20,21]. This is likely due to changes in the DG milieu, as neurotrophic factors and signaling molecules that stimulate the proliferation of NSCs decline in concentration with aging[22–25]. Moreover, other factors that are considered detrimental for neurogenesis also emerge in the aged hippocampus. These include chronic mild inflammation manifesting in the form of hypertrophy of astrocytes and activation of microglia[26,27], decreased availability of astrocyte-derived pro-neurogenic factors[23,28] and decreased microvasculature[29]. From this perspective, drugs having ability for restraining inflammation and enhancing microvasculature in the aged hippocampus are likely beneficial for stimulating quiescent NSCs to produce new neurons in the aged hippocampus. Increased neurogenesis and microvasculature and reduced inflammation may help in the maintenance of adequate memory and mood function in the normal elderly population.

Administration of resveratrol (RESV), a naturally occurring polyphenol found in high concentrations in the skin of red grapes, appears suitable for counteracting age-related detrimental changes in the hippocampus because of its pro-angiogenic and antiinflammatory properties with no adverse side effects[30–33]. Indeed, RESV has been shown to mediate a wide range of biological activities including extension of the life span and delayed onset of age related diseases[31,34–36]. Furthermore, RESV readily crosses the blood brain barrier and its activity in the brain lasts for up to 4 hrs[37]. Additionally, recent studies provide evidence that RESV intake in healthy older persons improves memory performance[38] and RESV has antidepressant effects in an animal model of depression[39]. Therefore, in this study, we rigorously examined the efficacy of intraperitoneal administration of RESV for maintaining/improving cognitive and mood function in aged male F344 rats. To understand mechanisms, we also investigated whether RESV therapy can increase neurogenesis and microvasculature, and modulate the hypertrophy of astrocytes and activation of microglia, in the aged hippocampus.

Results

Two groups of rats in late middle age (21-month old) chosen for the study displayed similar ability for spatial learning and memory formation. Figure 1 illustrates the time-line of treatment, behavioral tests and other analyses. Characterization using a water maze test (WMT) revealed that the two groups of 21-months old rats chosen for this study exhibited similar learning and memory ability prior to the commencement of treatment regimen (Fig. 2). Animals assigned to both groups also exhibited similar swim speed ($p > 0.05$, $F = 3.73$, Fig. 2 [A1]) across learning sessions. Two-way repeated measures analyses of variance (RM-ANOVA) revealed progressive and comparable decreases in latencies to reach the platform over seven training sessions in both groups ($p < 0.0001$, $F = 9.66$, Fig. 2 [A2]). Hence, learning curves did not differ between the two groups ($p > 0.05$, $F = 2.23$, Fig. 2 [A2]). Analyses of swim path efficiency (i.e. the ratio of the shortest possible swim path length to actual swim path length) demonstrated that both groups displayed comparable improvement in swim path efficiency values over seven learning sessions ($p < 0.0001$, $F = 7.2$) and hence their swim path efficiency curves were similar ($p > 0.05$, $F = 0.55$, Fig. 2 [A3]). Analyses of data from memory retrieval test performed 24 hours after the last learning session also showed similar results (Fig. 2 [B1–C1]). Animals in both groups showed a clear affinity for the platform quadrant (PQ, the quadrant where platform was placed during learning sessions), which was evidenced through considerably greater dwell time in PQ, in comparison to all other quadrants ($p < 0.05$–0.001, $F = 6.5$–9.2, one-way ANOVA, Fig. 2 [B2, B3]). Additional parameters such as dwell times in PQ and platform area (PA, a smaller area within the PQ denoting the actual position of the platform and an immediate surrounding region) and platform area crossings were also similar between the two groups ($p > 0.05$, Fig. 2 [C1–C3]).

RESV treatment in late middle age improved ability for spatial learning and spatial memory formation at an advanced age. The two groups of rats described above received either vehicle (VEH) or RESV for four weeks when they were in the 23rd month of their life. A month later (i.e. in 25th month of their life), a second WMT was performed to assess their ability to make new spatial memories. Animals belonging to both VEH and RESV groups learned to locate the position of submerged platform during training sessions. Two-way RM-ANOVA showed that there were no differences in swim speeds between the two groups ($p > 0.05$, $F = 0.3$, Fig. 3 [A1]). Furthermore, progressive decreases in latencies to reach the platform over training sessions were seen in both groups ($p < 0.0001$, $F = 12.27$, Fig. 3 [A2]). However, learning curves differed

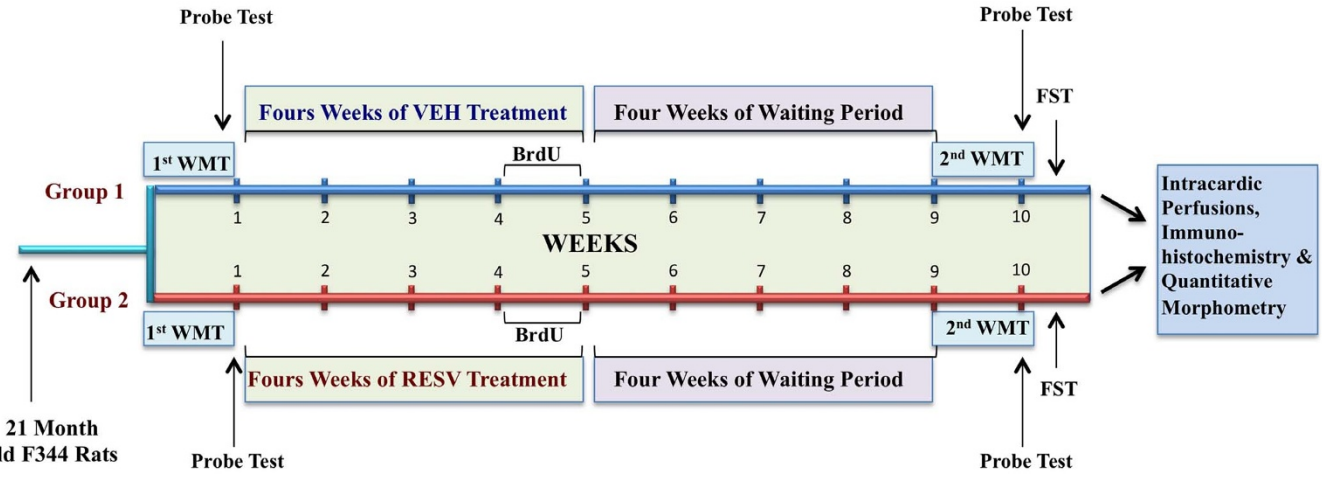

Figure 1 | A cartoon depicting the time-line of various experiments. A cohort of 21-months old rats was examined using a water maze test (WMT) and animals with normal spatial learning and memory function were chosen and divided into two groups. One of the groups then received vehicle (VEH, n = 7) and the other group received resveratrol (RESV, n = 8) for four weeks. Animals in both groups also received 5′-bromodeoxyuridine (BrdU) in the last week of VEH or RESV treatment to facilitate the labeling and quantification of newly born cells and neurons. Both groups underwent a second WMT four weeks after the termination of VEH or RESV treatment followed by a forced swim test (FST). Animals were next euthanized via intracardiac perfusions and brain tissues processed for immunohistochemical staining and various quantifications.

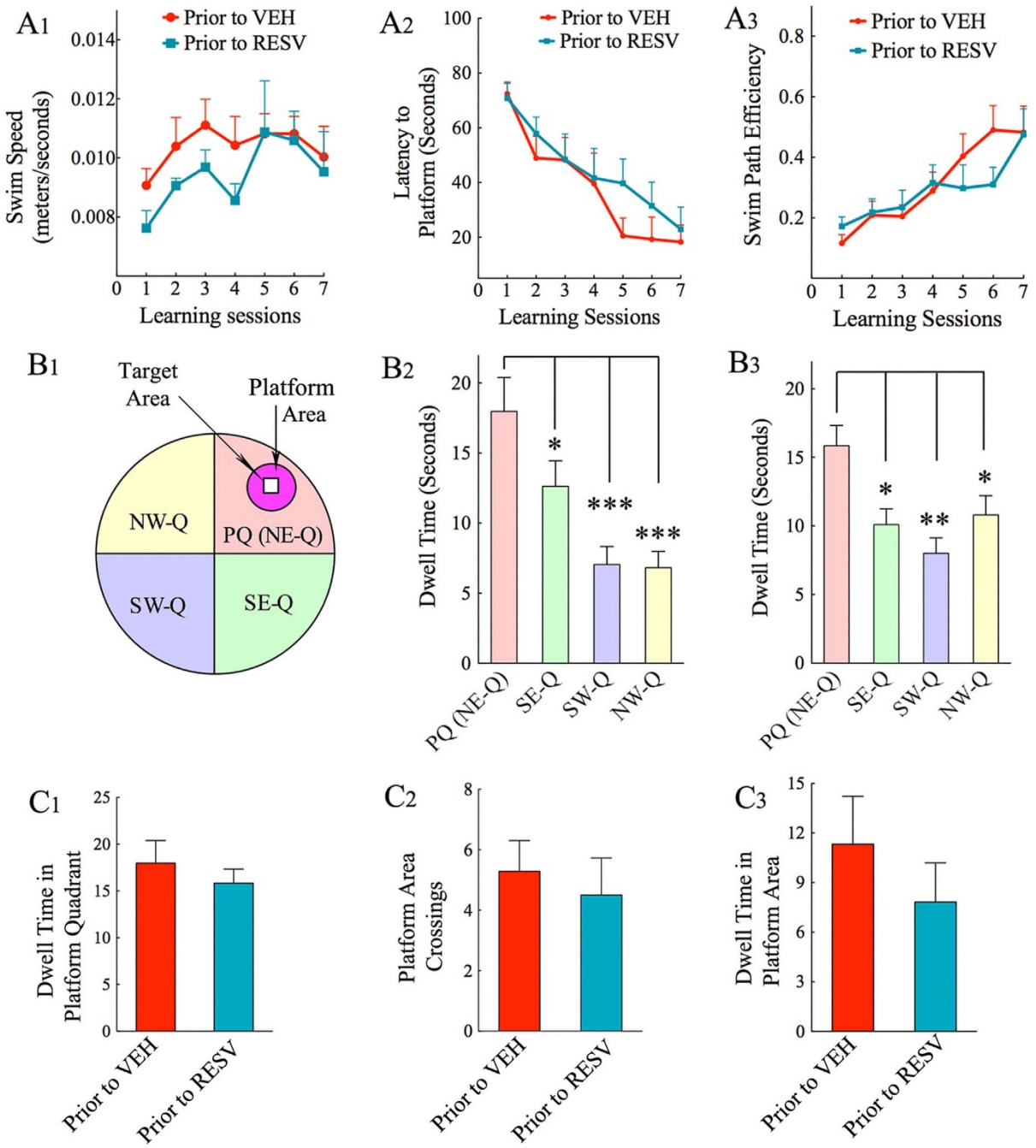

Figure 2 | Spatial learning and memory performance comparison between the two 21-months old animal groups chosen for vehicle (VEH, n = 7) or resveratrol (RESV, n = 8) treatment. There were no differences between the two groups for swim speed (A1; $p > 0.05$, two-way ANOVA), latencies to reach the platform (A2; $p > 0.05$) or swim path efficiency (A3; $p > 0.05$) in different learning sessions. Probe test conducted 24 hours after the last learning session revealed similar results (B1–B3). Both groups chosen for VEH (B2) or RESV (B3) treatment showed greater affinity for the platform quadrant, in comparison to the other three quadrants of the pool (one-way ANOVA, $p < 0.05$–0.001). Additional parameters of memory retrieval ability such as the dwell time in the platform quadrant (C1), platform area crossings (C2) and dwell time in platform area (C3) were also comparable between the two groups ($p > 0.05$). PQ (NE-Q), platform quadrant (northeast quadrant); SE-Q, southeast quadrant; SW-Q, southwest quadrant; and NW-Q, northwest quadrant. *, $p < 0.05$, **; $p < 0.01$; ***; $p < 0.001$.

significantly between the two groups ($p < 0.0001$, $F = 204.17$, Fig. 3 [A2]) because RESV-treated rats displayed much superior learning. This was evidenced through considerably shorter latencies to reach the platform in all learning sessions in RESV-treated aged rats, in comparison to VEH-treated aged rats ($p < 0.001$–0.0001). Swim path efficiency curves also differed significantly between RESV- and VEH-treated groups ($p < 0.001$, $F = 60.53$, Fig. 3 [A3]). In comparison to VEH-treated rats, RESV-treated rats displayed significantly greater swim path efficiency values for all learning sessions except session 6 ($p < 0.05$–0.01). Thus, RESV-treated rats displayed much superior ability for spatial learning than VEH-treated rats. Analyses of data from the memory retrieval test performed 24 hours after the last learning session demonstrated impaired ability in VEH-treated rats but preserved ability for spatial memory formation in RESV-treated rats (Fig. 3 [B1–C3]). Aged rats treated with VEH displayed no affinity for PQ over other quadrants in the probe test ($p > 0.05$, $F = 1.54$, Fig. 3 [B1, C1]). In contrast, aged rats treated with RESV demonstrated greater

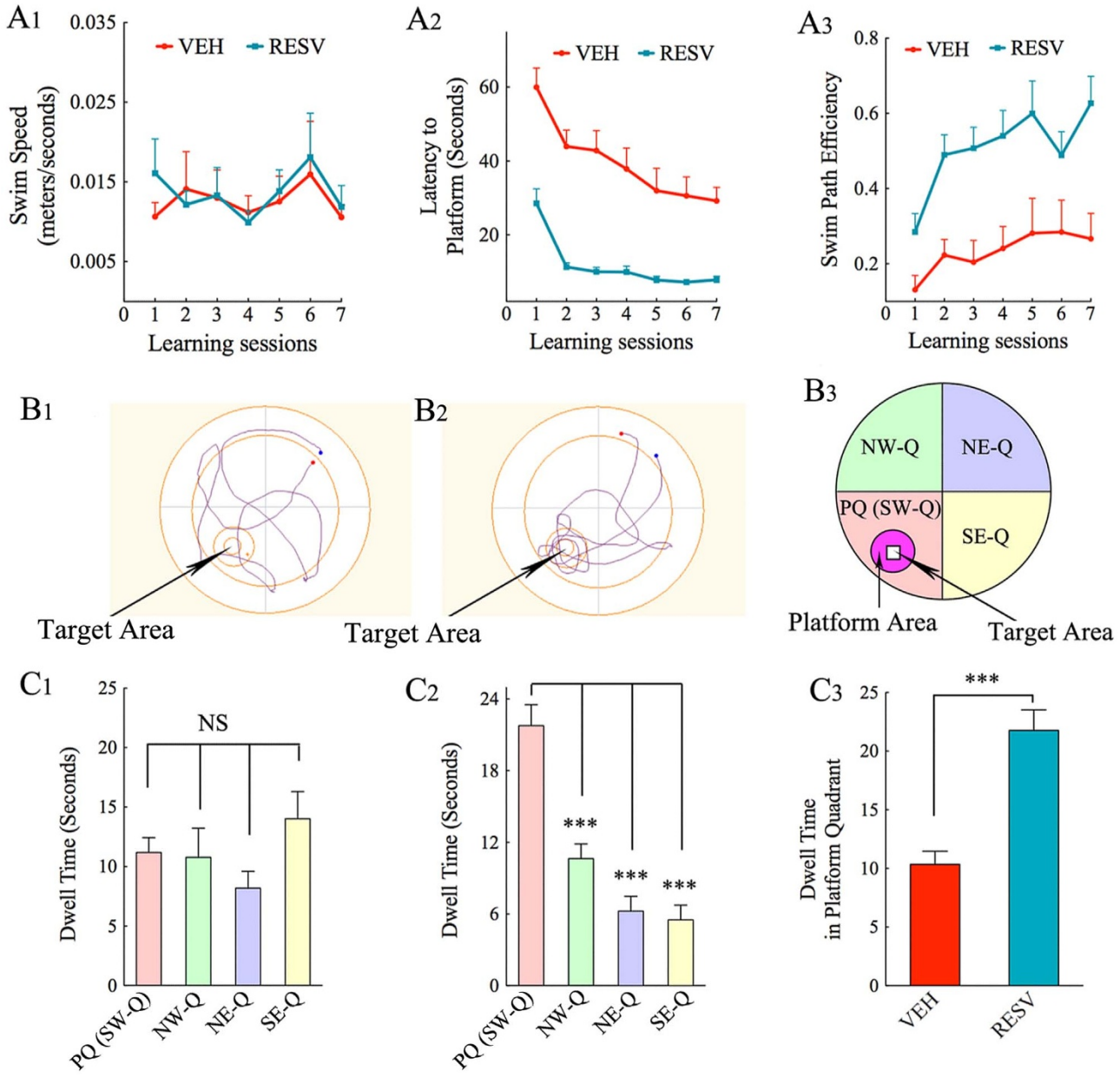

Figure 3 | Spatial learning and memory performance comparison between the vehicle (VEH, n = 7) treated and resveratrol (RESV, n = 8) treated animal groups, in the second water maze test performed four weeks after the termination of VEH or RESV treatment. Swim speeds were comparable between the two groups (A1; $p > 0.05$, two-way ANOVA) and both groups displayed ability for spatial learning (A2; $p < 0.0001$, repeated measures ANOVA). However, RESV treated rats displayed much superior learning than VEH treated rats (A2; $p < 0.0001$, two-way ANOVA) and this was also revealed through much improved swim path efficiency values in RESV treated animals (A3; $p < 0.001$). B1 and B2 illustrate swim paths of representative rats from VEH (B1) and RESV (B2) groups in a single-trial probe test conducted 24 hours after the last learning session whereas, figure B3 shows the position of four quadrants, the platform area and the target area in the water maze pool during the probe test. Note that, VEH treated rats showed almost equal affinity for all four quadrants (B1 and C1; $p > 0.05$, one-way ANOVA), implying memory retrieval dysfunction in these rats. In contrast, RESV treated rats exhibited a clear affinity for the platform quadrant over all other quadrants (B2, C2; $p < 0.001$). This difference is also apparent from a direct comparison of the dwell time in the platform quadrant across the two groups (C3; $p < 0.001$, two-tailed, unpaired Student's t-test). PQ (SW-Q), platform quadrant (southwest quadrant); NW-Q, northwest quadrant; NE-Q, northeast quadrant; SE-Q, southeast quadrant. ***, $p < 0.001$.

dwell times in the PQ, in comparison to all other quadrants (one-way ANOVA, $p < 0.0001$; post-hoc tests, $p < 0.001$, $F = 29.30$, Fig. 3 [B2, C2]). Direct comparison of dwell times in the PQ also showed clear differences between RESV- and VEH-treated groups ($p < 0.001$, Fig. 3 [C3]).

Analyses of spatial learning data between pre- and post-treatment periods in the VEH group showed that spatial learning ability neither improved nor worsened between 22 and 25 months of age. At both time-points, rats displayed similar progressive decreases in latencies to reach the platform ($p < 0.0001$, $F = 11.2$, Fig. 4 [A1]) and hence learning and swim path efficiency curves remained comparable ($p > 0.05$, $F = 0.14–1.7$, Fig. 4 [A1, A2]). Nonetheless, these rats lost ability for spatial memory formation by 25 months of age, which was evidenced through their lack of affinity towards PQ in the memory retrieval test conducted after the second WM training ($p > 0.05$, $F = 1.54$, Fig. 3 [C1]). Direct comparison revealed significantly reduced dwell times of these rats in PQ in the probe test performed after the second WMT ($p < 0.05$, Fig. 4 [A3]). In contrast, RESV-

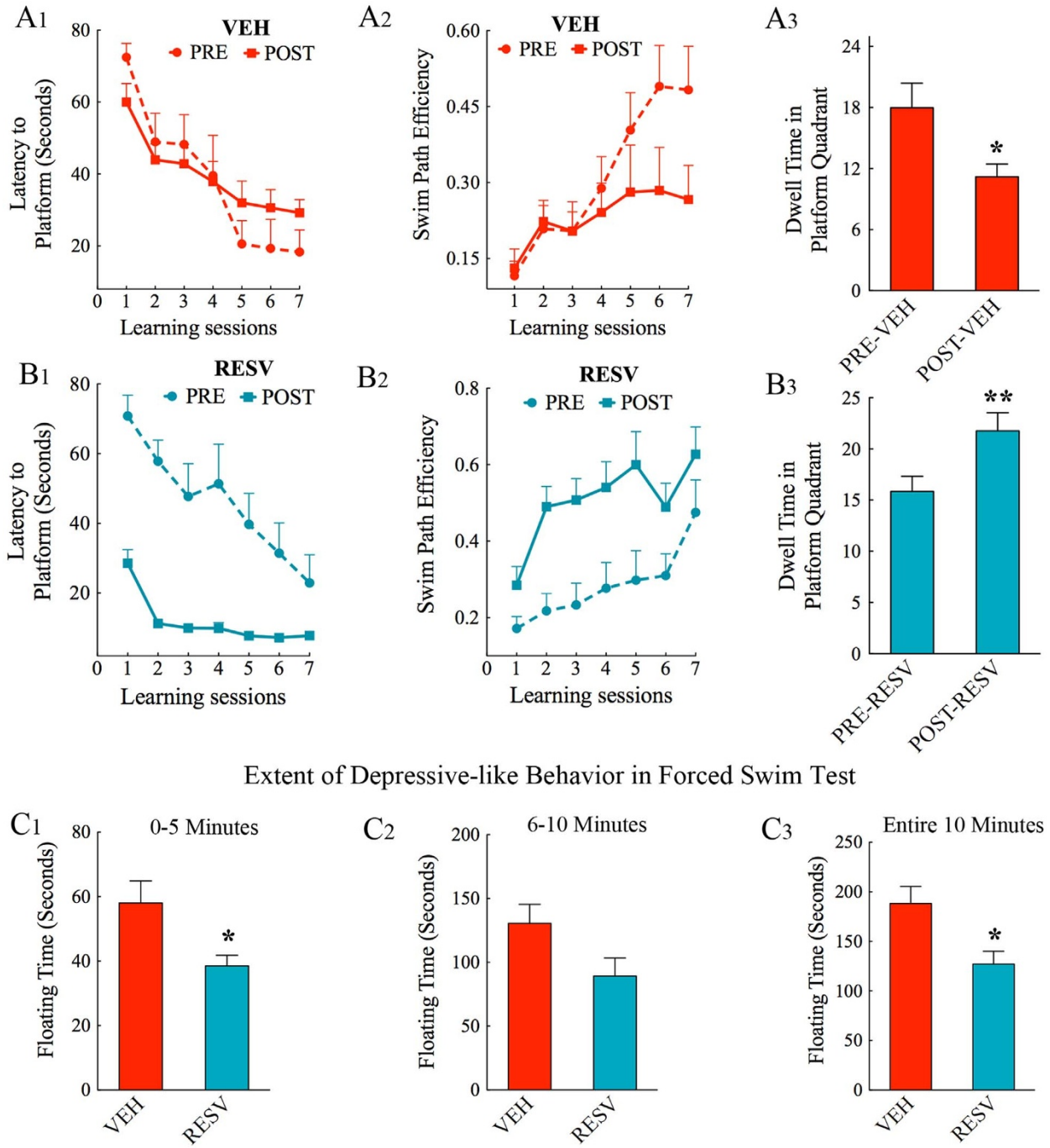

Figure 4 | Pre- and post-treatment spatial learning and memory performance comparison in vehicle (VEH, n = 7) and resveratrol (RESV, n = 8) treated aged rats. Rats treated with VEH retain the ability for spatial learning at pre-treatment levels, which is evident from their learning curves (A1; $p > 0.05$, two-way ANOVA) and swim path efficiency values (A2; $p > 0.05$). However, they exhibit memory retrieval dysfunction (A3; $p < 0.05$). In contrast, RESV treated rats display improved ability for spatial learning and memory retention in comparison to their pre-treatment performance. This is obvious from comparison of pre- and post-RESV treatment learning curves (B1, $p < 0.0001$), swim path efficiency values (B2; $p < 0.01$) and dwell time in the platform quadrant (B3; $p < 0.01$). (C1–C3): Comparison of depressive-like behavior in a forced swim test between VEH treated and resveratrol (RESV) treated aged rats. Note that, RESV treated aged rats displayed reduced depressive-like behavior, in comparison to VEH treated aged rats. The differences in floating time (or immobility) during the test were significant for the first five minutes of the test (C1; $p < 0.05$) as well as for the entire duration of the test (C3; $p < 0.05$) but not significant for the last 5 minutes of the test (C2; $p > 0.05$, two-tailed, unpaired Student's t-test). *, $p < 0.05$, **; $p < 0.01$.

treated aged animals displayed improved spatial learning performance. This was revealed through superior curves for learning ($p < 0.0001$, $F = 35.18$, Fig. 4 [B1]) as well as swim path efficiency in the post-treatment period ($p < 0.01$, $F = 12.3$, Fig. 4 [B2]). These rats also showed improved ability for spatial memory formation, which was seen through further increases in their affinity for PQ versus other quadrants ($p < 0.01$ in the probe test conducted after the first WM training, Fig. 2 [B2]; $p < 0.0001$ in the probe test conducted after the second WM training, Fig. 3 [C2]). Additionally, direct comparison showed increased dwell times of RESV-treated rats in PQ, in the probe test performed after the second WM training ($p < 0.05$, Fig. 4 [B3]). Thus, in the absence of therapeutic treatment, aged rats can maintain their spatial learning ability but lose their capacity for making new spatial memory between 22 and 25 months of age. In

contrast, with RESV treatment, aged rats showed an improved ability for both spatial learning and spatial memory during this period.

To further investigate the improved learning ability displayed by aged animals after RESV-treatment (i.e. in the second WMT), we compared latencies to reach the platform between the four trials performed on day 1 (i.e. the first learning session). While, RM-ANOVA analysis did not show statistically significant decreases in latency values ($p > 0.05$, $F = 2.3$), the overall percentage reductions in latency values over four trials suggested improved learning ability. Latency values were decreased by 55% between trials 1 and 2, 59% between trials 2 and 3 and 47% between trials 3 and 4 (Table 1 in supplement document). In contrast, VEH-treated animals did not show percentage decreases between trials 1 and 2 or 3 and 4, and showed only 22% decrease between trials 2 and 3 ($p > 0.05$, $F = 0.37$; Table 1 in supplement document). Thus, an improved learning ability of RESV-treated aged rats could be observed in the very first learning session. Furthermore, to examine whether overnight forgetting underlies impaired memory retrieval function in VEH-treated animals, we performed additional analyses on their spatial learning parameters. First, we compared the last trial (trial 4 or T4) latency values in every learning session (S) with the first trial (T1) latency values of the subsequent learning session (Table 2 in supplement document). Next, we compared average latency values of each of sessions 1–6 with T1 latency values of the subsequent learning session (T1 of S2–S7, Table 3 in supplement document). Both of these analyses did not imply the occurrence of overnight forgetting during learning in VEH-treated animals (Tables 2 and 3 in supplement document). However, their overall latency values decreased over seven learning sessions as they continuously improved their learning in subsequent learning sessions.

From their behavior, it appeared that RESV-treated animals remembered the logistics involved in finding the hidden platform from the first WMT (performed prior to treatment) better than VEH-treated animals. This was apparent from their ability to quickly locate the hidden platform by the second learning session, which allowed stronger memory encoding to occur in the remaining learning sessions (i.e. in learning sessions 3–7, Fig. 3 [A2]). This is in sharp contrast to VEH-treated rats, which showed progressive decreases in latency values over seven learning sessions but ended up having much higher latency values than RESV treated animals even in the 7th session of learning (Fig. 3 [A2]). Thus, VEH-treated animals remained in the learning phase over 7 sessions of learning whereas RESV-treated animals learned to quickly locate the platform within the first two sessions of learning and utilized the remaining sessions of learning for memory encoding.

RESV treatment did not alter motor function in VEH or RESV treated aged rats. Comparison of swim speeds of animals belonging to VEH and RESV treated groups across pre- and post-treatment periods revealed no differences in swim speeds ($p > 0.05$, Fig. 1 in supplement document). Thus, VEH or RESV treatment did not significantly alter the motor ability of aged rats. We did not perform visible platform test following spatial learning and memory test in this study as animals belonging to both VEH and RESV groups showed ability for spatial learning in both first and second WMTs. Hence, it is unknown whether RESV treatment improved vision function of aged rats in this study. Additional studies are needed in the future on possible RESV-mediated vision improvements in aged rats.

RESV treatment improved mood function in aged rats. Analyses of immobility (or floating) time in a forced swim test (FST) was used as a measure of depressive-like behavior in VEH and RESV treated rats, as rats with normal mood function are known to spend reduced amounts of the test time in floating. In the first five minutes of the test, RESV-treated aged rats spent reduced amount of time in floating than VEH-treated aged rats (34% reduction, $p < 0.05$, Fig. 4 [C1]). A similar trend was also observed in the final five minutes of the test (32% reduction, $p > 0.05$, Fig. 4 [C2]). When floating times for the entire 10 minutes duration were compared, it was clear that RESV-treated rats displayed decreased tendency for floating (127.2 ± 12.9 seconds) than VEH-treated aged rats (188.2 ± 17.2 seconds, $p < 0.05$, Fig. 4 [C3]). Thus, RESV treatment to aged rats resulted in an anti-depressant effect, implying improved mood function. However, as only FST was used for measuring depressive-like behavior in this study, additional behavioral tests measuring depression will be required in future studies to confirm the anti-depressive effects of RESV in aged rats.

RESV treatment enhanced net neurogenesis in the hippocampus of aged rats. Quantification of the total number of 5′-bromodeoxyuridine (BrdU) positive cells revealed increased addition of newly born cells to the subgranular zone-granule cell layer (SGZ–GCL) of aged rats receiving RESV treatment, in comparison to aged rats receiving VEH treatment (Fig. 5 [A1–G]). The addition of new cells was increased by 1.8-folds with RESV treatment ($p < 0.05$; Fig. 5 [E]). Quantification of fractions of newly born cells that differentiate into NeuN-expressing neurons in the SGZ-GCL (using dual immunofluorescence and confocal microscopy, Fig. 5 [C1–D3]) suggested no significant difference in neuronal differentiation of newly born cells between VEH and RESV-treated aged animals ($p > 0.05$, Fig. 5 [F]). Through extrapolation of BrdU+ cell numbers with the percentage of newly born cells expressing neuron-specific nuclear antigen (NeuN), we calculated net neurogenesis value for each animal and compared between the two groups. This analysis showed that RESV treatment to aged rats induced 2.4-folds increase in net hippocampal neurogenesis ($p < 0.01$, Fig. 5 [G]). Since BrdU injections were given during the last 7 days of RESV treatment, these results showed the extent of neurogenesis occurring in the 4th week of RESV treatment.

RESV treatment promoted increased neurogenesis in aged rats for prolonged periods. We also analyzed neurogenesis through quantification of neurons positive for doublecortin (DCX, a marker of newly born neurons) in the SGZ-GCL (Fig. 6 [A1–D]). Since DCX expression in newly born neurons lasts for ~2 weeks after their birth in F344 rats[40], this analyses provided a measure of ongoing neurogenesis. Aged rats treated with RESV exhibited 2.1 folds increase in DCX+ newly born neurons than aged rats receiving VEH ($p < 0.001$, Fig. 6 [D]). Since these neurons are generated ~6 weeks after the termination of RESV treatment, the results suggest that RESV treatment can trigger sustained increase in neurogenesis in the aged hippocampus even after its termination.

RESV treatment enhanced microvasculature in the hippocampus of aged rats. To determine whether RESV treatment improved cerebral blood flow, we measured microvasculature in the hippocampus using rat endothelial cell antigen-1 (RECA-1) immunostaining (Fig. 7 [A1–D4]). Area fraction analyses demonstrated increased microvasculature in RESV-treated rats, in comparison to VEH-treated rats (Fig. 7 [D1–D4]). The increase was significant for the CA1 subfield and the entire hippocampus ($p < 0.05$–0.01, Fig. 7 [D2, D4]).

RESV treatment reduced the hypertrophy of astrocytes in aged rats. Immunohistochemical staining for glial fibrillary acidic protein (GFAP) suggested increased occurrence of astrocytes with hypertrophy in VEH-treated rats, in comparison to RESV-treated rats (Fig. 7 [E1–G2]). Therefore, we measured the area fraction of GFAP+ astrocyte elements (soma and processes) in different subfields of the hippocampus. This quantification revealed reduced astrocyte hypertrophy in the hippocampus of RESV-treated aged rats. The reductions varied from 42 to 45% for different subfields of the hippocampus ($p < 0.001$, Fig. 7 [H1–H3]). When the

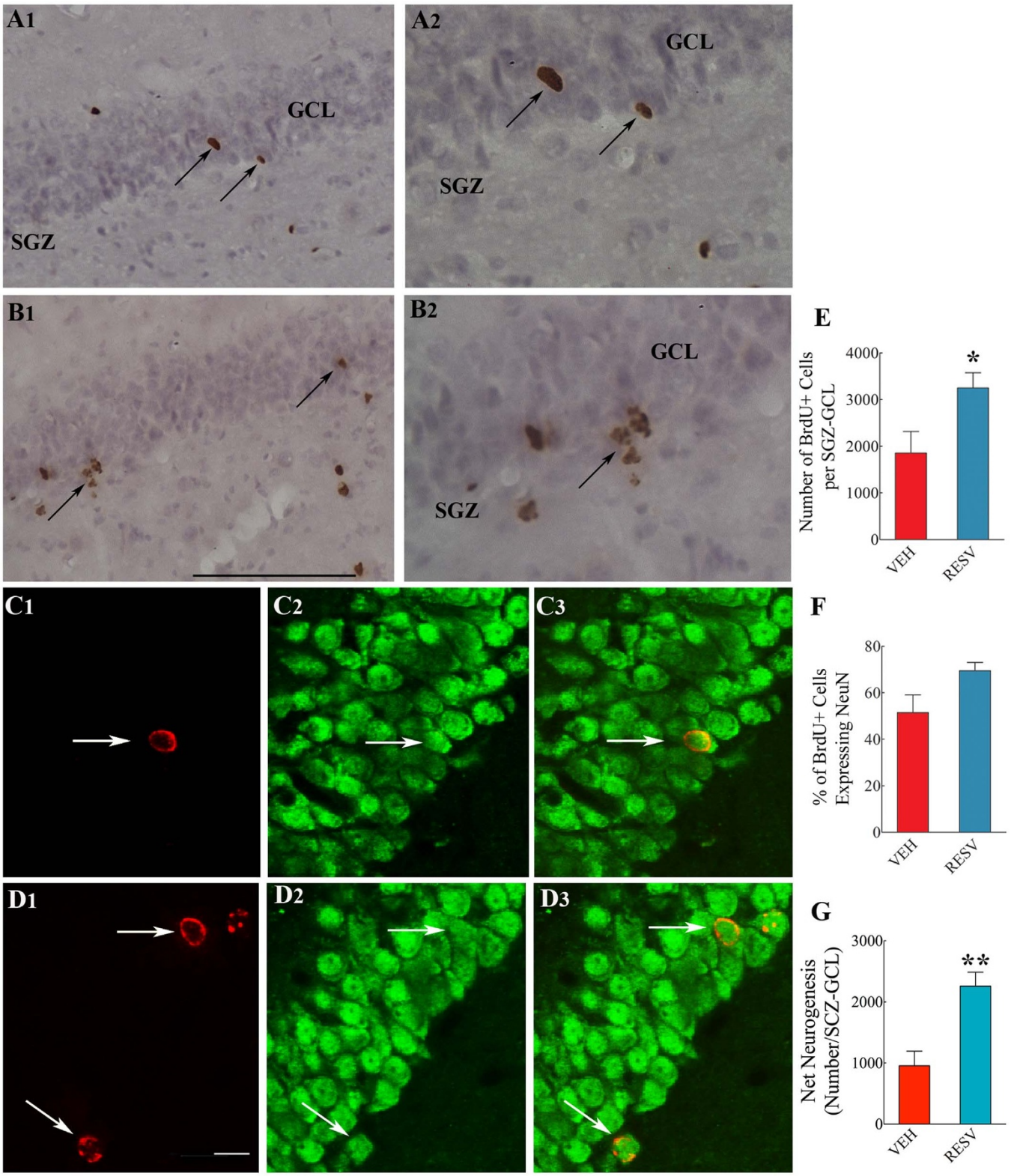

Figure 5 | Examples of newly born cells expressing 5′-bromodeoxyuridine (BrdU) in the subgranular zone-granule cell layer (SGZ-GCL) of the hippocampus from a rat that received vehicle (VEH) treatment (A1) and a rat that received resveratrol (RESV) treatment (B1). (B1 and B2) are magnified views of regions from A1 and B1. Figures (C1–D3) show examples of BrdU+ newly born cells that mature and express neuron specific nuclear antigen (NeuN). Bar charts compare numbers of newly born (BrdU+) cells (E), percentages of newly born cells expressing NeuN (F) and net hippocampal neurogenesis (G) between VEH and RESV treated groups (n = 6/group). Note that, both numbers of newly born cells and net hippocampal neurogenesis are greater in RESV treated rats than VEH treated rats ($p < 0.05$–0.01, two-tailed, unpaired, Student's t-test). *, $p < 0.05$, **; $p < 0.01$. Scale bar, A1 and B1, 100 μm; A2 and B2, 50 μm; C1–D3, 10 μm.

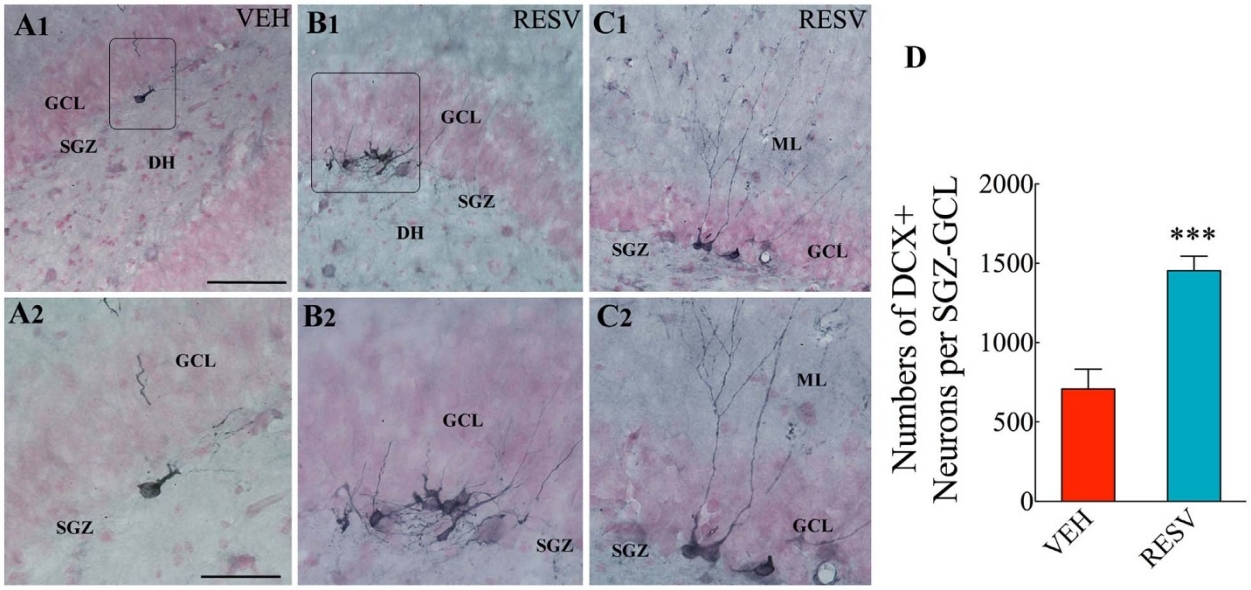

Figure 6 | Newly born neurons expressing doublecortin (DCX) in the subgranular zone-granule cell layer (SGZ–GCL) of rats treated with vehicle (VEH; A1) or resveratrol (RESV; B1, C1). (A2, B2 and C2) are magnified views of regions from (A1, B1 and C1). Comparison of numbers of DCX+ newly born neurons between VEH and RESV treated groups (bar chart in D, n = 6/group) revealed greatly enhanced production of newly born neurons in RESV treated aged animals ($p < 0.001$, two-tailed, unpaired Student's t-test). DH, dentate hilus; ML, molecular layer. Scale bar, (A1, B1 and C1), 100 μm; (A2, B2 and C2), 50 μm. ***, $p < 0.001$.

hippocampus was taken in entirety, the overall decrease was 44% ($p < 0.001$, Fig. 7 [H4]).

RESV treatment reduced activation of microglia in aged rats. Immunohistochemical characterization using OX-42 (CD11b) antibody revealed increased occurrence of activated microglia displaying enlarged soma and fewer processes in VEH-treated rats, resulting in larger spaces between microglia (Fig. 8 [A1, B1, C1]). In contrast, RESV-treated rats showed mostly ramified microglia (i.e. resting microglia exhibiting very extensive fine processes) (Fig. 8 [A2, B2, C2]). Hence, we quantified the area fraction of OX-42+ microglial elements (soma and processes) in the hippocampus. This measurement suggested increased occurrence of ramified or resting microglia in RESV-treated rats than VEH-treated rats (Fig. 8 [D1–D4]) and differences were significant for the CA1 subfield and the entire hippocampus ($p < 0.05$, Fig. 8 [D2, D4]). To confirm this further, we performed tracing of OX-42+ microglia and its processes from both VEH- and RESV-treated groups using Neurolucida (Fig. 8 [E1, E2]). This quantification showed that, in comparison to microglia in VEH-treated aged rats, microglia in RESV-treated animals displayed 25% greater numbers of segments in their processes ($p < 0.05$, Fig. 8 [F1]) and 35% greater total process length ($p < 0.05$, Fig. 8 [F2]). Furthermore, the concentric circle analysis of Sholl revealed that, microglia from RESV-treated aged rats exhibited greater numbers of intersections at 0-10 μm and 20–30 μm distances from the soma (Fig. 8 [F3]), and greater number of process endings at 0–50 μm distance from the soma, in comparison to microglia from VEH-treated aged rats ($p < 0.05$, Fig. 8 [F4]). These results implied that most microglia in RESV-treated rats have highly ramified appearance whereas considerable numbers of microglia in the VEH-treated aged rats have modified into activated microglia with fewer processes. To authenticate this possibility further, we performed immunostaining for ED-1 (CD68, a specific marker of activated microglia exhibiting amoeboid morphology) and quantified the numbers of ED-1+ cells in the DG (Fig. 9 [A1–C]). This showed that VEH-treated rats contained 29% greater numbers of activated microglia than RESV-treated aged rats ($p < 0.05$, Fig. 9 [C]). Collectively, these results confirmed that RESV-treatment in old age reduced the presence of activated microglia in the hippocampus.

RESV treatment did not alter the volume of hippocampus. To ascertain the effects of RESV treatment on hippocampus volume, we measured the volume of hippocampus in animals belonging to both VEH and RESV groups. This analysis revealed that both VEH- and RESV-treated animals exhibited comparable hippocampal volumes (VEH group, Mean ± SEM = 27.57 ± 1.01 mm^3, RESV group, 27.79 ± 1.63 mm^3, $p > 0.05$). Thus, the beneficial effects mediated by RESV did not change the overall volume of hippocampus.

Discussion

The results of this study in a rat model of aging provide new evidence that RESV treatment in late middle age can positively modulate the structure and function of the aged hippocampus. The structural changes that occurred with RESV treatment comprised increased neurogenesis and microvasculature, and reduced astrocyte hypertrophy and activation of microglia. The beneficial functional effects included improved ability for spatial learning, preserved proficiency for making new spatial memory, and alleviation of depressive-like behavior associated with aging. Because decreases in neurogenesis and microvasculature, and increases in astrocyte hypertrophy and activation of microglia during aging can adversely affect cognitive and mood function, the structural plasticity mediated by RESV in the aged hippocampus have likely contributed greatly towards beneficial functional effects.

Rationale for using RESV for mitigating age-related cognitive, memory and mood dysfunction. Decline in cognitive capacity after middle age is seen in most humans as well as in animal models. In humans, this may manifest in the form of occasional forgetfulness, decreased processing speed and mental flexibility, and reduced ability for solving problems or maintaining attentiveness[41]. Although these problems in milder forms are typical for the elderly population, progression of these snags into a measurable decline in cognition and memory would result in a

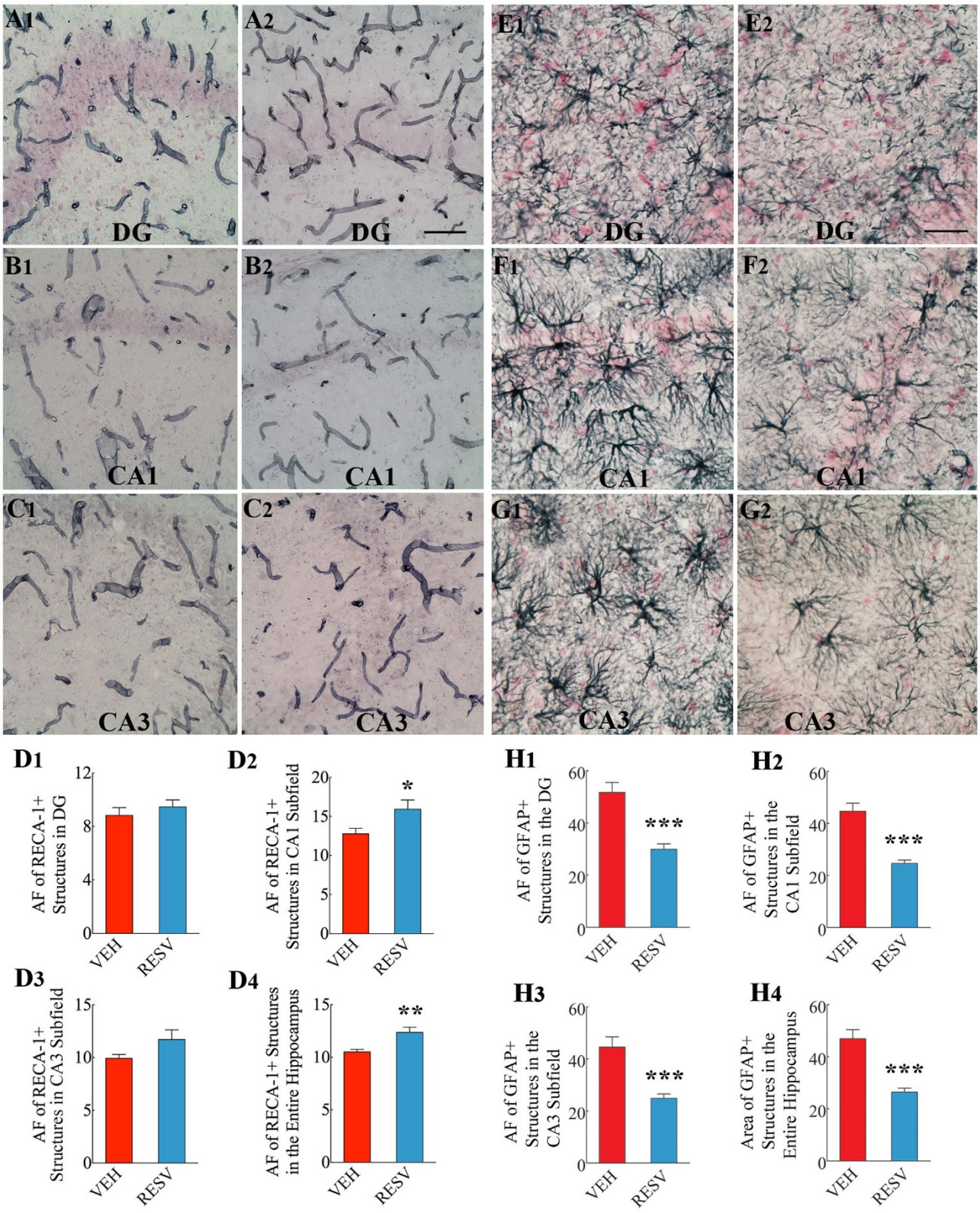

Figure 7 | Distribution of rat endothelial cell antigen-1 (RECA-1)-positive microvessels and glial fibrillary acidic protein (GFAP)-positive astrocytes in vehicle (VEH) and resveratrol (RESV) treated groups. (A1–C2) compare the distribution of RECA-1+ microvessels in the dentate gyrus (DG, A1, A2), the CA1 subfield (B1, B2) and the CA3 subfield (C1, C2) of the hippocampus between VEH treated (A1, B1, C1) and RESV treated (A2, B2, C2) animals. Bar charts in D1–D4 compare area fraction of RECA-1+ structures in different regions of the hippocampus between the two groups (n = 6/group). Note that, RESV treatment increased the area fraction of RECA-1+ structures in the CA1 subfield and the entire hippocampus (D2, D4; $p < 0.05$–0.01, two-tailed, unpaired Student's t-test). (E1–G2) compare the distribution and morphology of GFAP+ astroctyes in the DG (E1, E2), the CA1 subfield (F1, F2) and the CA3 subfield (G1, G2) of the hippocampus between VEH treated (E1, F1, G1) and RESV treated (E2, F2, G2) animals. Bar charts (H1–H4) compare area fraction of GFAP+ structures in different regions of the hippocampus between the two groups (n = 6/group). Note that, RESV treatment considerably decreased the area fraction of GFAP+ structures in all subfields of the hippocampus as well as for the entire hippocampus (H1–H4, $p < 0.001$). Scale bar, (A1–C2 and E1–G2), 25 μm. *, $p < 0.05$, **; $p < 0.01$; ***; $p < 0.001$.

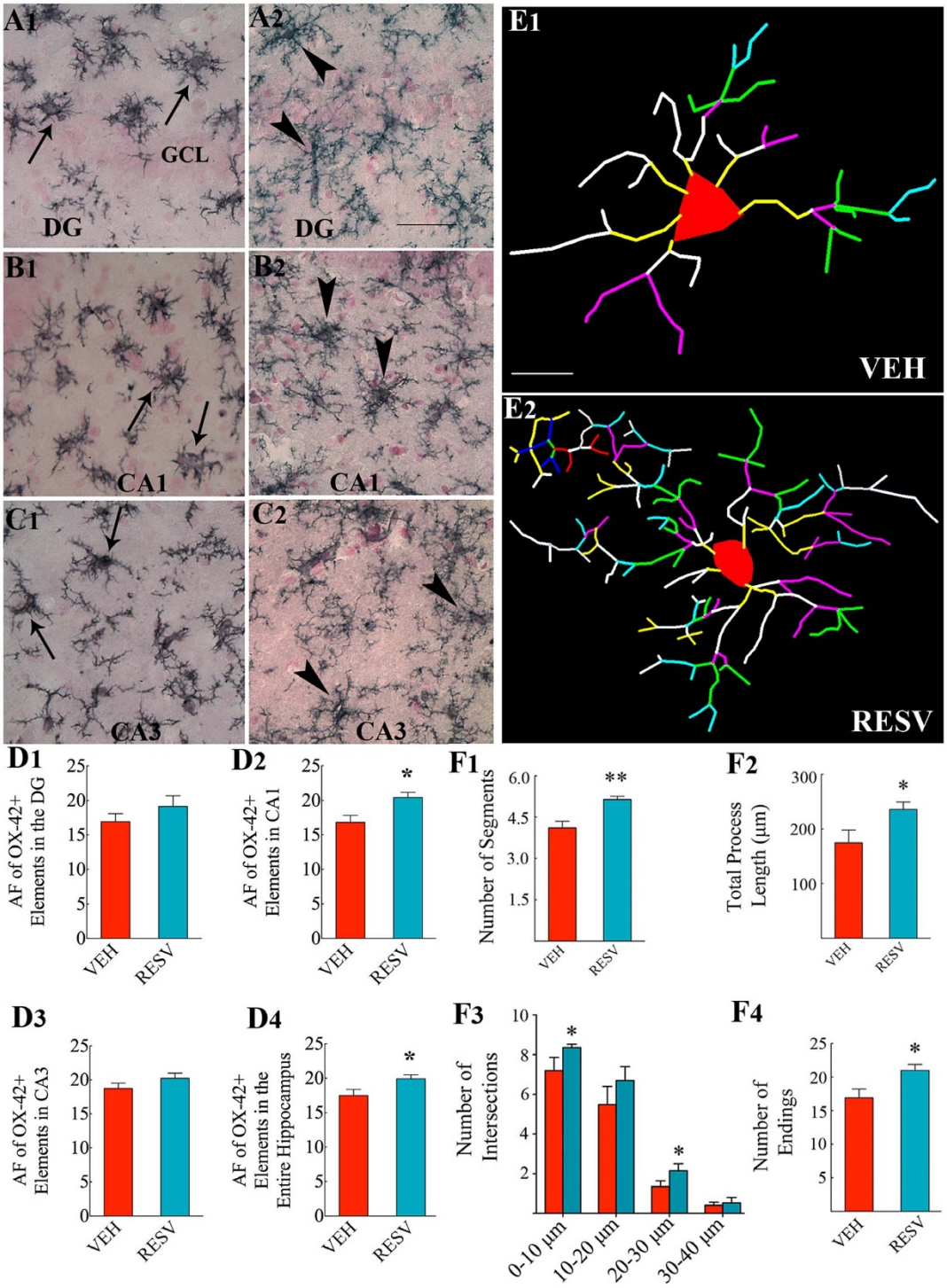

Figure 8 | Distribution of OX-42 (CD11b)-positive microglia in the hippocampus of vehicle (VEH) and resveratrol (RESV) treated groups. (A1–C2) compare the distribution and morphology of OX-42+ microglia in the dentate gyrus (DG, A1, A2), the CA1 subfield (B1, B2) and the CA3 subfield (C1, C2) of the hippocampus between VEH treated (A1, B1, C1) and RESV treated (A2, B2, C2) animals. E1 and E2 show representative examples of microglial morphology traced with Neurolucida from VEH treated (E1) and RESV treated (E2) rats. Most microglia in VEH-treated aged rats exhibited enlarged soma, shorter processess and reduced ramification of processes (arrows in A1, B1, C1, and the cartoon in E1), implying a tendency towards conversion into amoeboid or activated microglia. In contrast, most microglia in RESV treated rats maintained longer processes with extensive ramifications (arrowheads in A2, B2, C2, and the cartoon in E2) suggestive of resting microglia. Bar charts in (D1–D4) compare area fraction of OX-42+ structural elements in different regions of the hippocampus between the two groups (n = 7/group). RESV treatment increased the area fraction of OX-42+ structures in the CA1 subfield and the entire hippocampus (D2, D4; $p < 0.05$, two-tailed, unpaired Student's t-test). Bar charts in (F1–F4) compare the number of segments (F1), the total process length (F2), the number of intersections (F3) and the number of process endings (F4) in microglia traced from VEH and RESV treated aged animals (n = 42 microglia/group). Note that RESV treated animals displayed greater numbers of segments (F1, $p < 0.01$), increased process length (F2, $p < 0.05$), increased numbers of intersections at 0–10 μm and 20–30 μm distances from the soma (F3, $p < 0.05$), and greater numbers of process endings (F4, $p < 0.05$). Scale bar, (A1–C2 and E1–G2), 25 μm; (E1–E2), 10 μm. *, $p < 0.05$, **; $p < 0.01$.

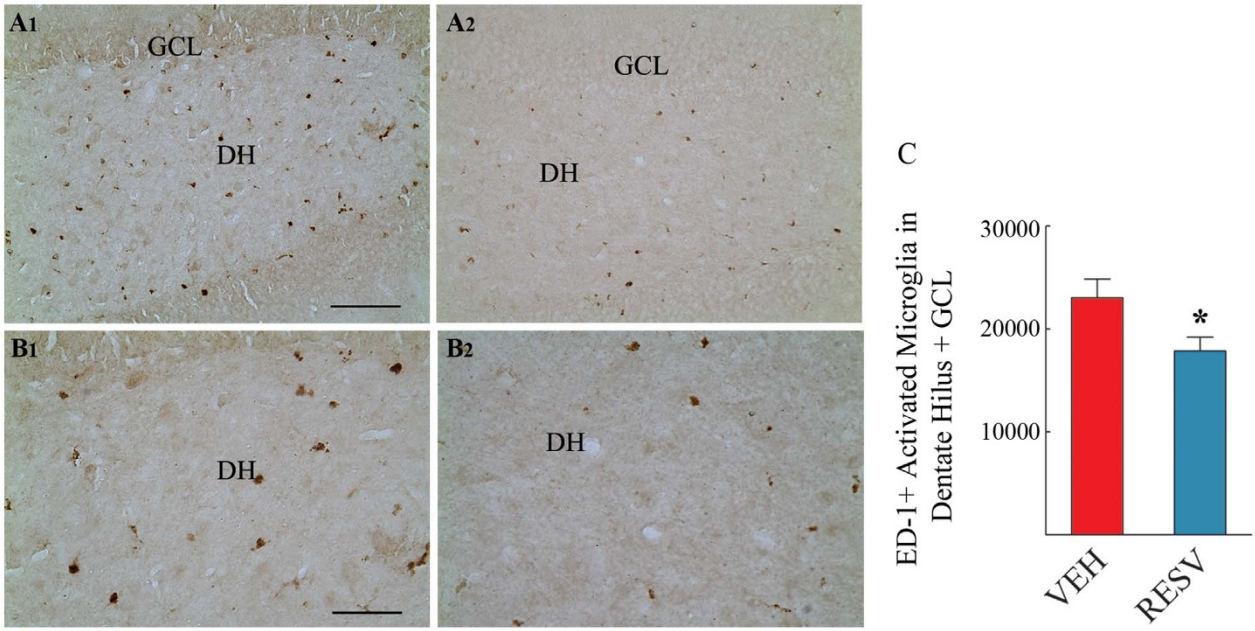

Figure 9 | Distribution of ED-1 (CD68)-positive activated microglia in the dentate hilus (DH) and granule cell layer (GCL) of vehicle (VEH, A1) and resveratrol (RESV, A2) treated groups. (B1 and B2) are magnified views of dentate hilar regions from A1 and B2. The bar chart in C compares numbers of ED-1+ activated microglia between VEH and RESV treated rats (n = 6/group). Values represent means and standard errors. Note that, the RESV treated group exhibited decreased numbers of ED-1+ activated microglia than the VEH treated group ($p < 0.05$, two-tailed, unpaired Student's t-test). Scale bar, (A1–A2), 100 μm; (E1–E2), 50 μm. *, $p < 0.05$.

clinical condition called MCI. Because people with MCI have an increased risk for developing AD or other type of dementia[2], interventions that can improve cognitive and memory function in old age or prevent MCI in old age have immense importance. A multitude of factors including myelin loss, thinning of the cerebral cortex, decreased hippocampus volume, reduced neurotransmitter concentrations, altered neuronal networks associated with decreases in neuron size and synaptic density can contribute to cognitive decline with aging[41,42]. On the other hand, memory and mood dysfunction in old age has been linked strongly to decreased function of DG in the hippocampus[3,4]. There are several structural changes in the aged DG that parallel its diminished function. Greatly reduced neurogenesis is one of the conspicuous alterations attracting the most attention because of its purported role in learning, memory and mood function[6,14,13,20]. Additional structural changes in the DG include diminished ability of interneurons to synthesize the inhibitory neurotransmitter gamma-amino butyric acid (GABA) resulting in compromised inhibitory synaptic transmission[43,44], and loss of synapses between DG granule cells and perforant path afferents from the entorhinal cortex[42]. However, these changes are likely secondary to multiple primary age-related alterations in the DG. These include decreased blood flow due to loss of microvasculature, endothelial cell dysfunction or plaques in cerebral blood vessels[29], increased oxidative stress[45], chronic low-level inflammation in the form of hypertrophy of astrocytes and activation of microglia[26,27], and reduced concentration of astrocyte-derived pro-neurogenic and pro-angiogenic factors and signaling molecules[22–25,28]. If the above proposition is true, then, therapeutic interventions that reverse one or more of the primary age-related changes in the brain should improve cognitive and mood function in the aged population. Indeed, several earlier studies have shown that administration of nutraceuticals having ability to suppress oxidative stress and/or inflammation or low-doses of antiepileptic drugs capable of increasing GABA-ergic neurotransmission can improve memory function in aging rodents[44,46–48].

We chose RESV in this study because of its ability to readily cross the blood-brain barrier following peripheral administration, promote angiogenesis, suppress oxidative stress, inflammation and mitochondrial dysfunction, activate longevity genes and extend life span without adverse side effects[31–35,37]. Moreover, RESV treatment can mimic caloric restriction, a strategy that has been found to exert several beneficial effects on the aging brain[49,50]. Furthermore, previous studies have shown that RESV treatment can provide protection against neurodegeneration in models of AD[51], improve cognitive function in adult primates[52] and enhance hippocampal microvasculature in aging mice[53]. In addition, recent studies report that RESV treatment can improve memory performance in healthy older persons[38] and promote antidepressant effects in an animal model of depression[39]. Our goal was to determine whether short-term RESV treatment in late middle age can improve cognitive and mood function in old age and whether any improvements in cognitive and mood function seen with RESV treatment will be associated with improved neurogenesis and microvasculature and/or suppression of chronic low-level inflammation typically seen in the aged hippocampus.

Mechanisms underlying RESV-mediated improvements in learning, memory and mood function in aged rats. To understand mechanisms underlying RESV-mediated beneficial effects on learning, memory and mood, we quantified the extent of neurogenesis, microvasculature, astrocyte hypertrophy and activation of microglia in the hippocampus. These are measures that are known to undergo alterations in old age and substantial changes in them can adversely influence memory and mood. First, it is clear that aging is associated with greatly waned hippocampal neurogenesis, and memory and mood dysfunction in aging can be attributed at least partially to greatly decreased neurogenesis. This is because: (i) increased hippocampal neurogenesis in middle-aged and aged animals exposed to enriched environment is allied with increased ability for making new spatial memories[17,18]; (ii) aged rats having ability for forming new spatial memories display higher levels of hippocampal neurogenesis than impaired aged rats[54,55]; (iii) middle-aged mice exercising on running wheels or having lowered stress hormone levels demonstrate both enhanced hippocampal neurogenesis and better memory ability[15,16];

(iv) aged rats displaying ability for making new spatial memories exhibit enhanced survival of new cells generated just prior to the onset of learning[56]; and (v) progenitor cells in the hippocampus of depressed patients exhibit decreased proliferation than age-matched controls[19]. Second, it has been demonstrated in earlier studies that aging is associated with degenerative changes in cerebral capillaries causing decreased microvasculature, reduced blood flow, disruption of the blood-brain barrier and increased infiltration of CD45+ macrophages in the hippocampus[29,57]. It is believed that these changes in microvasculature contribute to memory dysfunction in aging[29,57]. Third, chronic low-level inflammation is one of the conspicuous features of the aged rodent and human hippocampus[58], which can be gauged through changes in the morphology of astrocytes and microglia. Astrocytes in the aged hippocampus display reactive phenotype and a significant fraction of microglial cells in the aged hippocampus undergoes activation. This kind of chronic low-level inflammation in the aged hippocampus can adversely affect memory and mood function. For example, systemic inflammation induced pro-inflammatory changes in the hippocampus causes deficits in the hippocampal long-term potentiation (LTP, a basis of learning and memory) in middle-aged rats and antiinflammatory therapy restores LTP in these rats[59].

Interestingly, RESV treatment enhanced net neurogenesis in the last week of RESV treatment, and maintained increased neurogenesis and microvasculature when examined at ~25 months of age (i.e. ~6 weeks after the termination of RESV treatment). Furthermore, RESV treatment had antiinflammatory effects in the form of reduced hypertrophy of astrocytes and diminished activation of microglia. The microvasculature enhancing effects of RESV noted here is consistent with earlier findings that RESV treatment improves endothelial function and cerebral blood flow[60,61], whereas its antiinflammatory effects are in line with a previous study showing that RESV can reduce plasma levels of pro-inflammatory cytokines[62]. On the other hand, neurogenesis-enhancing effects of RESV in the aged hippocampus are likely mediated through increased microvasculature and suppression of inflammation in the neurogenic niche (i.e. SGZ of the DG), as both decreased vasculature/blood flow and inflammation can adversely affect the proliferation of NSCs and neurogenesis[63].

Thus, the precise reasons underlying a diminished spatial learning ability and an impaired memory function in VEH-treated aged animals and improved spatial learning and memory ability in RESV-treated aged rats are unknown. However, as age-related memory dysfunction typically occurs between 18 and 24 months of age in male F344 rats[64], it is plausible that impaired spatial learning and memory function in VEH-treated animals is linked to multiple adverse changes in the aged hippocampus that are detailed above. Additional age-related changes observed in earlier studies such as alterations in dendritic morphology, cellular connectivity, gene expression and other factors affecting plasticity and network dynamics of neural ensembles supporting cognition and memory may also be involved[65]. On the other hand, improved memory retrieval function in RESV-treated animals is likely owed to multiple RESV-mediated beneficial changes, which may include increased neurogenesis and microvasculature and dampened inflammation described above. Several molecular mechanisms are expected to be involved in mediating these beneficial changes. These could comprise increased expression of SIRT1 (nicotinamide adenine dinucleotide-dependent histone deacetylase), a longevity factor that undergoes upregulation with RESV treatment and is believed to play a role in the maintenance of normal cognitive and mood function and neurogenesis[66,67]. Indeed, a parallel study in our laboratory has shown that four weeks of oral RESV treatment to aged rats increased the expression of SIRT1 gene as well as its down-stream target FOXO3[68], a transcription factor that regulates the capacity of cells to cope with endoplasmic reticulum and oxidative stress[69]. Furthermore, alteration in the expression of nuclear factor kappa B (NF-kB), a transcription factor responsible for the regulation of multiple target genes related to inflammation, could be involved in the suppression of inflammation, as RESV treatment has been shown to modulate NF-kB pathways in several models[70,71]. In addition, activation of adenosine monophosphate (AMP) activated protein kinase (AMPK), a protein kinase having a major role in neuronal differentiation and mitochondrial biogenesis in neurons, may also be involved, as RESV is known to up-regulate AMPK in a SIRT1-dependent manner[66]. Furthermore, mechanisms such as an improved glucose metabolism and enhanced functional connectivity between the posterior hippocampus and the medial prefrontal cortex observed in a recent human study[38], reduction in serum corticosterone and regulation of the hypothalamus-pituitary-adrenal (HPA) axis[72] and enhanced brain-derived neurotrophic factor (BDNF) signaling pathway[39,73] may also be contributing to RESV-mediated improved cognitive and mood function. Studies on these aspects at different time-points after RESV treatment in aging models will be needed in the future to understand their role.

Another remarkable attribute of this study is that improved cognitive function in aged rats following RESV treatment differed from an earlier study on the effects of RESV treatment in juvenile (4-weeks old) mice[74]. This study showed that administration of RESV to juvenile mice reduced hippocampal neurogenesis as well as cognitive function, in association with activation of AMPK and down-regulation of the phosphorylated form of cyclic AMP response element-binding protein (pCREB) and BDNF in the hippocampus. The discrepancy reflects divergent effects of RESV on the juvenile vis-à-vis the aged brain. Administration of RESV in the juvenile age corresponds to a time when the hippocampus was still maturing with very high levels of neurogenesis. This is in sharp contrast to the current study where RESV was administered at a time when the aged hippocampus was exhibiting a greatly declined neurogenesis, reduced cerebral blood flow, chronic low level inflammation and increased oxidative stress. It is likely that inflammation, oxidative stress and reduced cerebral blood flow in the aged brain contributed to the reduced neurogenesis and impaired cognitive function and RESV treatment enhanced neurogenesis and microvasculature through antiinflammatory, antioxidant and pro-angiogenic effects, which in turn improved cognitive function in aged rats. On the other hand, since the juvenile brain does not normally display inflammation, increased oxidative stress or decreased cerebral blood flow, RESV-mediated suppression of normal levels of oxidative stress that are believed to be required for neural stem cell (NSC) proliferation and differentiation[75] may have impaired neurogenesis and interfered with the cognitive function in juvenile mice. The observed opposing effects of RESV on the juvenile vis-à-vis the aged brain also imply that RESV treatment can have beneficial effects in a background of a disease state or in conditions such as aging, but may adversely affect function of the developing or the young brain[74]. Additional longitudinal studies over the lifespan of animals will be useful to comprehend the mechanisms underlying these differences. Nonetheless, the beneficial effects of RESV treatment for the aged brain is also apparent from a recent human study, which demonstrated that lower dose of RESV intake for 26 weeks can improve memory performance as well as hippocampus functional connectivity in healthy but overweight older individuals[38]. Additionally, our study on the effects of oral administration of a higher dose of RESV (90 mg/Kg) is supportive, which showed that preserved memory function in aged rats receiving RESV was associated with increased expression of multiple genes encoding cognitive function and neurotrophic factors[68].

Conclusions

Our results in a rat model of aging provide novel evidence that four weeks of daily RESV treatment in late middle age is efficacious for improving cognitive, memory and mood function in old age. Additional analyses demonstrated that improved cognitive and

mood function following RESV treatment is linked with amelioration of several age-related changes such as decreased neurogenesis and microvasculature and low-level chronic inflammation in the hippocampus. These results suggest that RESV therapy in middle age is beneficial for maintaining normal memory and mood function in old age.

Methods

Animals and research design. Twenty-one month old male Fischer 344 rats acquired from Harlan Sprague-Dawley (Indianapolis, IN, USA) were used in this study. All experiments were performed as per the animal protocol approved by the animal studies subcommittee of the Durham Veterans Affairs Medical Center. Following arrival, animals were allowed to have 7–10 days acclimatization in the vivarium. Animals for this study were chosen from a larger cohort of aged rats (n = 80) that were screened for hippocampus-dependent spatial learning and memory ability using Morris WMT[76] for several different studies in the laboratory. Figure 1 illustrates the time-line of various treatments and analyses. Animals with normal spatial learning and memory function were chosen and divided into two groups. One of the groups then received daily intraperitoneal injections of RESV (n = 8, 40 mg/Kg dissolved in 0.5 ml of 2% ethyl alcohol, Sigma-Aldrich, St. Louis, MO, USA) while the other group received daily intraperitoneal injections of VEH solution (n = 7) for four weeks. The dose of RESV was based on findings in our preliminary studies using middle-aged rats, where this dose increased hippocampal neurogenesis. We chose intraperitoneal injections in this study because we wanted to examine the effects of a relatively lower dose of RESV for a shorter duration (4 weeks). The drug was injected into areas in the left or right halves of the peritoneal cavity alternatively to minimize repeated injections at one site and peritoneal irritation. Following injections, animals were closely monitored and no writhing behavior was observed. Thus, animals did not show signs of dermal or peritoneal irritation because of very lower concentration of alcohol used as vehicle in this study.

In order to label newly born cells and neurons in the hippocampus animals in both groups also received BrdU (100 mg/kg) injections during the last 7 days of RESV treatment. A month after RESV treatment, a fresh round of WMT was conducted. Following this, the extent of depressive-like behavior was quantified using an FST. In order to determine the production of new cells and the status of hippocampus neurogenesis, stereological quantifications of cells positive for BrdU and DCX were performed for the SGZ-GCL of the DG using serial sections (every 10th) immunostained for BrdU or DCX and StereoInvestigator (Microbrightfield Inc., Williston, VT, USA). Furthermore, to ascertain net hippocampus neurogenesis, analyses of BrdU$^+$ cells expressing NeuN were carried out for the SGZ-GCL using confocal microscopy and Z-section analyses. To determine the effects of RESV on other structural changes in different subfields (DG, CA1 and CA3) of the hippocampus, we also quantified areas occupied by the microvasculature, astrocytes and microglia through immunohistochemical staining of serial sections (every 15th through the hippocampus) for RECA-1 (a marker of cerebral blood vessels), GFAP (a marker astrocytes), OX-42 (a marker of microglia) and area fraction analyses using J Image. Moreover, to distinguish any changes in the morphology, we quantified processes of microglia using Neurolucida (Microbrightfield). Additionally, to quantify the fraction of microglia that was activated in the vicinity of the neurogenic region, we performed ED-1 immunohistochemistry using serial sections (every 15th) and quantified the numbers of activated microglia in the DG using StereoInvestigator.

Analyses of hippocampus-dependent spatial learning and memory function. Hippocampus-dependent spatial learning and memory function in aged rats was analyzed using a WMT, as described in our recent studies[77,78]. A circular water maze tank (measuring 170 cm in diameter and 75 cm in height) was filled with water at room temperature to 35 cm height. The water was rendered opaque by the addition of a white, non-toxic paint, and extra-maze cues were positioned on the walls of the room around the tank. The pool was arbitrarily divided into four equal quadrants and a circular platform (15 cm diameter) was submerged 1 cm below the water surface in the middle of one quadrant. A quartz halogen lamp was positioned aiming at the ceiling to indirectly illuminate the water surface. A video camera was mounted on the ceiling directly above the center of the pool and the movement of rat in the water maze tank was continuously video-tracked and recorded using a computerized ANY-Maze video tracking system (Stoelting ANY-maze, Wood Dale, IL, USA). The rat was trained to find the platform using spatial cues for 7 sessions over 7 days with 4 acquisition trials per session. Each rat was placed in the water, immediately facing the wall of the tank in one of the quadrants in pseudo-random manner, and then allowed a maximal time of 90 seconds to locate the platform with an inter-trial interval of 120 seconds. Each trial commenced from a different start location. When the subject reached the platform it was allowed to stay there for 30 seconds. When the subject failed to find the platform within the ceiling time of 90 seconds, it was guided onto the platform and allowed to stay there for 30 seconds. The platform was positioned in the same place across all sessions. Data such as the latency and swim path lengths to reach the platform, swim path efficiency (the ratio of the shortest possible swim path length to actual swim path length), and swim speed were collected using Anymaze software. Mean latencies to reach the platform were used for assessment of learning curves, as swim speeds did not differ between groups in this study. A day after the 7-day learning protocol described above, each rat was subjected to a single 45-second probe or memory retrieval test. This involved removal of the platform from the pool and release of rats from the quadrant that is diametrically opposite to the quadrant where the platform was positioned during learning sessions. Retrieval of learned memory was assessed by comparing dwell time in the PQ with the other three quadrants within the group and also by comparing dwell time in platform quadrant, latency to reach the platform area, dwell time in platform area and platform area crossings across groups.

Characterization of depressive-like behavior. An FST was employed for assessing depressive-like behavior in aged rats (n = 7–8/group), as the validity of FST as a measure of depressive-like behavior has been suggested in many previous studies[79,80]. This test was done as detailed in our recent studies[78,81]. In brief, 24 hours after the completion of WMT, each rat was placed in an acrylic glass cylinder having a diameter of 18.7 cm and depth of 42 cm and containing room temperature (25°C) water to a depth of 30 cm. This ensured that the rat could not touch the bottom of the cylinder with its tail or hind paws or escape from the top. The rat was subjected to a single session of forced swimming lasting ten minutes. We directly performed the forced swimming trial, as this test was conducted two days after the completion of WMT. Since animals have experienced swimming during learning sessions in the WMT, a separate swimming trial was not given prior to testing in an FST. Animal behavior during the test was monitored and recorded by a video camera. Investigators scored immobility time for each animal using the recorded videos. Animals that exhibited signs of drowning behavior were quickly removed from the cylinder and excluded for FST analyses. The amount of time spent in immobility (also referred to as floating) was calculated later. Immobility is defined as the minimal movement necessary to keep the head above the water level. The amount of time spent in floating was used as a measure of depressive-like behavior and compared between groups (n = 5–6/group). Furthermore, we compared FST data in two separate segments (5 minutes each). This is because typically in the first 5 minutes of the test, normal animals (i.e. animals having no depression) tend to swim continuously with minimal time spent in immobility in contrast to depressed animals spending greater amount of time in immobility. In the last 5 minutes of the test, even a normal rat may display increased immobility due to swimming related fatigue. Therefore, analysis of two segments of FST time helps to dissociate depression-related immobility from fatigue-related immobility.

Tissue processing and immunohistochemistry. Animals underwent intracardiac perfusions with 4% paraformaldehyde solution prepared in phosphate buffer (PB). Each animal was first deeply anesthetized with isoflurane in a Plexiglas chamber until it ceased respiration. Following this, the chest was surgically opened, the heart was exposed, a nick was made in the right atrium, and sequentially infused with normal saline and 4% paraformaldehyde through the left ventricle. The brains were dissected, post-fixed overnight in 4% paraformaldehyde solution, washed in PB, and treated with different concentrations (10–30%) of sucrose until they sank to the bottom of the container. Each brain was then mounted on a cryostat chuck and 30-micrometer thick coronal sections through the hippocampus were cut and collected serially in 24-well plates. Two sets of serial sections (every 10th) through the entire hippocampus were picked from each animal belonging to RESV and VEH control groups and processed for BrdU and DCX immunostaining, as described in our previous studies[12,13,82,83]. In order to measure the fraction of BrdU+ cells that express the mature neuronal marker neuron-specific nuclear antigen (NeuN) in the SGZ-GCL, another set of serial sections (every 15th) through the hippocampus was processed for BrdU and NeuN dual immunofluorescence staining, as described in our earlier reports[84]. Furthermore, additional sets of serial sections (every 20th) through the hippocampus were processed for immunohistochemical characterization of cells positive for RECA-1[20], GFAP[23], OX-42[22] and ED-1[77]. The primary antibodies comprised monoclonal antibodies against BrdU (1 : 500, BD Biosciences, San Jose, CA, USA or 1 : 200, Serotech, Raleigh, NC, USA), NeuN (1 : 1000, EMD Millipore, Darmstadt, Germany), OX-42 (1 : 500, AbD Serotech), RECA-1 and ED-1 (1 : 1000, AbD Serotech), and polyclonal antibodies against DCX (1 : 250; Santa Cruz Biotechnology, Santa Cruz, CA, USA) and GFAP (1 : 2000, Dako, Carpinteria, CA, USA).

Stereological quantification of BrdU+ cells, DCX+ neurons and ED-1+ activated microglia. Numbers of BrdU+ newly born cells and DCX+ newly born neurons in the SGZ-GCL, and ED-1+ activated microglia in the entire DG, were stereologically measured using the optical fractionator method (n = 6 animals/group). For this, we used 30-micrometer thick serial sections (every 10th for BrdU and DCX and every 20th for ED-1 analyses) through the entire hippocampus and the StereoInvestigator system (Microbrightfield) comprising a color digital video camera (Optronics Inc., Muskogee, OK, USA) interfaced with a Nikon E600 microscope, as detailed in our earlier publications[40]. In brief, the contour of the chosen counting region (SGZ-GCL or the entire DG) was marked in every section, the optical fractionator component was activated, and the density and location of counting frames (each measuring 40 × 40 μm) and the counting depth were determined by entering parameters such as the grid size (75 μm), the thickness of top guard zone (4 μm) and the optical dissector height (i.e. 8 μm). A computer driven motorized stage then allowed the cells to be measured at each of the counting frame locations. In every location, the top of the section was set, and the plane of the focus was moved 4 μm deeper through the section (guard zone). This plane served as the first point of the counting process. All cells that came into focus in the next 8 μm section thickness were counted if they were entirely within the counting frame or touching the upper or right side of the counting frame. This procedure was repeated for all serial sections. By utilizing parameters such as the initial section thickness (i.e. at the time of sectioning), the section

thickness at the time of cell counting (i.e. after immunostaining), and cell counts from the counting frame locations, the StereoInvestigator program calculated the total number of BrdU+/DCX+/ED-1+ cells per SGZ-GCL or the entire DG, as described in our earlier studies[12,13]. The Gundersen coefficient error (CE) was in the range of 0.05–0.15 for all counts in this study.

Measurement of BrdU+ cells expressing the mature neuronal marker NeuN. The sections processed for BrdU and NeuN dual immunofluorescence were analyzed using a laser scanning confocal microscope (FV-10i, Olympus), as described in our earlier reports[84]. The Z-stacks taken at 1-μm intervals were analyzed for identification of cells dual labeled for BrdU and NeuN and the percentages of $BrdU^+$ cells expressing NeuN were computed.

Quantitative analyses of RECA-1+, GFAP+ and OX-42+ structures in the hippocampus. The areas occupied by RECA-1+ vascular, GFAP+ astrocyte, and OX-42+ microglial elements (area fractions) were measured per unit area of the tissue in the DG, and CA1 and CA3 subfields of the hippocampus, as described in our recent study[81]. This quantification was accomplished through Image J for Windows (n = 6–7 animals/group). In brief, microscopic images from different regions of the hippocampus were digitized using 20× objective lens in a Nikon E600 microscope equipped with a digital video camera connected to a computer. Each image saved in gray scale as a bitmap file was opened in Image J, and a binary image was created through selecting a threshold value that kept all RECA-1+/GFAP+/OX-42+ immunostained elements but no background. The area occupied by the RECA-1+/GFAP+/OX-42+ structures (area fraction) in the binary image was then measured by selecting the Analyze command in the program. Area fraction of RECA-1+/GFAP+/OX-42+ structures was calculated separately for every hippocampal region in each animal by using data from all chosen serial sections before the means and SEs were determined for the total number of animals included per group (n = 6–7).

Morphometry of microglia expressing OX-42. The overall morphology of microglia were compared between RESV and VEH treated groups by measuring processes of randomly selected but well stained OX-42 microglial cells from both groups. These measurements were made using a semiautomatic neuron tracing system (Neurolucida; Microbrightfield) linked to a Nikon microscope. In each group, forty-two $OX\text{-}42^+$ microglial cells (from 7 animals) were individually traced in their entirety using oil immersion 100× lens, and data for the number of processes and total process length were computed. To measure the extent of process growth away from the soma and the branching of processes at different distances from the soma, the concentric circle analysis of Sholl was performed using NeuroExplorer component of the Neurolucida program.

Measurement of the volume of hippocampus. The volume of hippocampus was measured through tracing of the outer margin of the hippocampus (including fimbria, n = 6 animals/group), using serial coronal brain sections (every 15th) through the entire hippocampus immunostained for DCX. A semiautomatic tracing system (Neurolucida, Microbrightfield) linked to a Nikon microscope was employed for these measurements.

Statistical analyses. All statistical analyses were done using Prism software. Data pertaining to spatial learning (latencies to reach the platform in successive learning sessions and swim path efficiency) were compared between groups using two-way RM-ANOVA followed by Bonferroni's multiple comparisons test. The major results of probe tests (e.g. dwell time in platform quadrant versus all other quadrants) were compared using one-way ANOVA followed by Newman-Keuls multiple comparisons test. All other data between the two groups were compared using unpaired, two-tailed, Student's t-test.

1. Maruszak, A. & Thuret, S. Why looking at the whole hippocampus is not enough-a critical role for anteroposterior axis, subfield and activation analyses to enhance predictive value of hippocampal changes for Alzheimer's disease diagnosis. *Front. Cell. Neurosci.* **8**, 95 (2014).
2. Bensadon, B. A. & Odenheimer, G. L. Current management decisions in mild cognitive impairment. *Clin. Geriatr. Med.* **4**, 847–871 (2013).
3. Small, S. A., Chawla, M. K., Buonocore, M., Rapp, P. R. & Barnes, C. A. Imaging correlates of brain function in monkeys and rats isolates a hippocampal subregion differentially vulnerable to aging. *Proc. Natl. Acad. Sci. U.S.A.* **101**, 7181–7186 (2004).
4. Pavlopoulos, E. *et al.* Molecular mechanism for age-related memory loss: the histone-binding protein RbAp48. *Sci. Transl. Med.* **5**, 200ra115 (2013).
5. Eriksson, P. S. *et al.* Neurogenesis in the adult human hippocampus. *Nat. Med.* **4**, 1313–1317 (1998).
6. Sahay, A. *et al.* Increasing adult hippocampal neurogenesis is sufficient to improve pattern separation. *Nature* **472**, 466–470 (2011).
7. Spalding, K. L. *et al.* Dynamics of hippocampal neurogenesis in adult humans. *Cell* **153**, 1219–1227 (2013).
8. Imayoshi, I. *et al.* Roles of continuous neurogenesis in the structural and functional integrity of the adult forebrain. *Nat. Neurosci.* **11**, 1153–1161 (2008).
9. Snyder, J. S., Soumier, A., Brewer, M., Pickel, J. & Cameron, H. A. Adult hippocampal neurogenesis buffers stress responses and depressive behavior. *Nature* **476**, 458–461 (2011).
10. Boldrini, M. *et al.* Hippocampal angiogenesis and progenitor cell proliferation are increased with antidepressant use in major depression. *Biol. Psychiatry.* **72**, 562–571 (2012).
11. Kuhn, H. G., Dickinson-Anson, H. & Gage, F. H. Neurogenesis in the dentate gyrus of the adult rat: age-related decrease of neuronal progenitor proliferation. *J. Neurosci.* **16**, 2027–2033 (1996).
12. Rao, M. S., Hattiangady, B., Abdel-Rahman, A., Stanley, D. P. & Shetty, A. K. Newly born cells in the ageing dentate gyrus display normal migration, survival and neuronal fate choice but endure retarded early maturation. *Eur. J. Neurosci.* **2**, 464–476 (2005).
13. Rao, M. S., Hattiangady, B. & Shetty, A. K. The window and mechanisms of major age-related decline in the production of new neurons within the dentate gyrus of the hippocampus. *Aging Cell* **6**, 545–558 (2006).
14. Lee, S. W., Clemenson, G. D. & Gage, F. H. New neurons in an aged brain. *Behav. Brain. Res.* **227**, 497–507 (2012).
15. van Praag, H., Shubert, T., Zhao, C. & Gage, F. H. Exercise enhances learning and hippocampal neurogenesis in aged mice. *J. Neurosci.* **25**, 8680–8685 (2005).
16. Montaron, M. F. *et al.* Lifelong corticosterone level determines age-related decline in neurogenesis and memory. *Neurobiol. Aging* **27**, 645–654 (2006).
17. Kempermann, G., Gast, D. & Gage, F. H. Neuroplasticity in old age: sustained fivefold induction of hippocampal neurogenesis by long-term environmental enrichment. *Ann. Neurol.* **52**, 135–143 (2002).
18. Speisman, R. B. *et al.* Environmental enrichment restores neurogenesis and rapid acquisition in aged rats. *Neurobiol. Aging* **34**, 263–274 (2013).
19. Lucassen, P. J., Stumpel, M. W., Wang, Q. & Aronica, E. Decreased numbers of progenitor cells but no response to antidepressant drugs in the hippocampus of elderly depressed patients. *Neuropharmacology* **58**, 940–949 (2010).
20. Hattiangady, B. & Shetty, A. K. Aging does not alter the number or phenotype of putative stem/progenitor cells in the neurogenic region of the hippocampus. *Neurobiol. Aging* **29**,129–147 (2008).
21. Lugert, S. *et al.* Quiescent and active hippocampal neural stem cells with distinct morphologies respond selectively to physiological and pathological stimuli and aging. *Cell Stem Cell* **6**, 445–456 (2010).
22. Shetty, A. K., Rao, M. S., Hattiangady, B., Zaman, V. & Shetty, G. A. Hippocampal neurotrophin levels after injury: Relationship to the age of the hippocampus at the time of injury. *J Neurosci. Res.* **78**, 520–532 (2004).
23. Shetty, A. K., Hattiangady, B. & Shetty, G. A. Stem/progenitor cell proliferation factors FGF-2, IGF-1, and VEGF exhibit early decline during the course of aging in the hippocampus: role of astrocytes. *Glia* **51**, 173–186 (2005).
24. Hattiangady, B., Rao, M. S., Shetty, G. A. & Shetty, A. K. Brain-derived neurotrophic factor, phosphorylated cyclic AMP response element binding protein and neuropeptide Y decline as early as middle age in the dentate gyrus and CA1 and CA3 subfields of the hippocampus. *Exp. Neurol.* **5**, 353–371 (2005).
25. Miranda, C. J. *et al.* Aging brain microenvironment decreases hippocampal neurogenesis through Wnt-mediated survivin signaling. *Aging Cell* **11**, 542–552 (2012).
26. Latour, A. *et al.* Omega-3 fatty acids deficiency aggravates glutamatergic synapse and astroglial aging in the rat hippocampal CA1. *Aging Cell* **12**, 76–84 (2013).
27. Kohman, R. A., Bhattacharya, T. K., Wojcik, E. & Rhodes, J. S. Exercise reduces activation of microglia isolated from hippocampus and brain of aged mice. *J. Neuroinflammation* **10**, 114 (2013).
28. Bernal, G. M. & Peterson, D. A. Phenotypic and gene expression modification with normal brain aging in GFAP-positive astrocytes and neural stem cells. *Aging Cell* **10**, 466–482 (2011).
29. Zhang, R., Kadar, T., Sirimanne, E., MacGibbon, A. & Guan, J. Age-related memory decline is associated with vascular and microglial degeneration in aged rats. *Behav. Brain Res.* **235**, 210–217 (2012) .
30. Manna, S. K., Mukhopadhyay, A. & Aggarwal, B. B. Resveratrol suppresses TNF-induced activation of nuclear transcription factors NF-kappa B, activator protein-1, and apoptosis: potential role of reactive oxygen intermediates and lipid peroxidation. *J. Immunol.* **164**, 6509–6519 (2000).
31. Baur, J. A. & Sinclair, D. A. Therapeutic potential of resveratrol: the in vivo evidence. *Nat. Rev. Drug Discov.* **5**, 493–506 (2006).
32. Shetty, A. K. Promise of resveratrol for easing status epilepticus and epilepsy. *Pharmacol. Ther.* **131**, 269–286 (2011).
33. Simão, F. *et al.* Pro-angiogenic effects of resveratrol in brain endothelial cells: nitric oxide-mediated regulation of vascular endothelial growth factor and metalloproteinases. *J. Cereb. Blood Flow. Metab.* **32**, 884–895 (2012).
34. Baur, J. A. *et al.* Resveratrol improves health and survival of mice on a high-calorie diet. *Nature* **444**, 337–342 (2006).
35. Orallo, F. Trans-resveratrol: a magical elixir of eternal youth? *Curr. Med. Chem.* **15**, 1887–1898 (2008).
36. Karuppagounder, S. S. *et al.* Dietary supplementation with resveratrol reduces plaque pathology in a transgenic model of Alzheimer's disease. *Neurochem. Int.* **54**, 111–118 (2009).
37. Wang, Q. *et al.* Resveratrol protects against global cerebral ischemic injury in gerbils. *Brain Res.* **958**, 439–447 (2002).
38. Witte, A. V., Kerti, L., Margulies, D. S. & Flöel, A. Effects of resveratrol on memory performance, hippocampal functional connectivity, and glucose metabolism in healthy older adults. *J. Neurosci.* **34**, 7862–7870 (2014).
39. Hurley, L. L., Akinfiresoye, L., Kalejaiye, O. & Tizabi, Y. Antidepressant effects of resveratrol in an animal model of depression. *Behav. Brain Res.* **268**, 1–7 (2014).

40. Rao, M. S. & Shetty, A. K. Efficacy of doublecortin as a marker to analyze the absolute number and dendritic growth of newly generated neurons in the adult dentate gyrus. *Eur. J. Neurosci.* **19**, 234–246 (2004).
41. Harada, C. N., Natelson Love, M. C. & Triebel, K. L. Normal cognitive aging. *Clin. Geriatr. Med.* **29**, 737–752 (2013).
42. Morrison, J. H. & Hof, P. R. Life and death of neurons in the aging cerebral cortex. *Int. Rev. Neurobiol.* **81**, 41–57 (2007).
43. Stanley, D. P. & Shetty, A. K. Aging in the rat hippocampus is associated with widespread reductions in the number of glutamate decarboxylase-67 positive interneurons but not interneuron degeneration. *J. Neurochem.* **89**, 204–216 (2004).
44. Koh, M. T., Haberman, R. P., Foti, S., McCown, T. J. & Gallagher, M. Treatment strategies targeting excess hippocampal activity benefit aged rats with cognitive impairment. *Neuropsychopharmacology* **35**, 1016–1025 (2010).
45. Serrano, F. & Klann, E. Reactive oxygen species and synaptic plasticity in the aging hippocampus. *Ageing Res. Rev.* **3**, 431–443 (2004).
46. Acosta, S. *et al*. NT-020, a natural therapeutic approach to optimize spatial memory performance and increase neural progenitor cell proliferation and decrease inflammation in the aged rat. *Rejuvenation Res.* **13**, 581–588 (2010).
47. Rodrigues, J. *et al*. Protective effects of a catechin-rich extract on the hippocampal formation and spatial memory in aging rats. *Behav. Brain Res.* **246**, 94–102 (2013).
48. Wang, H. M. *et al*. Neuroprotective effects of forsythiaside on learning and memory deficits in senescence-accelerated mouse prone (SAMP8) mice. *Pharmacol. Biochem. Behav.* **105**, 134–141 (2013).
49. Ingram, D. K., Young, J. & Mattison, J. A. Calorie restriction in nonhuman primates: assessing effects on brain and behavioral aging. *Neuroscience* **145**, 1359–1364 (2007).
50. Stranahan, A. M. & Mattson, M. P. Impact of energy intake and expenditure on neuronal plasticity. *Neuromolecular Med.* **10**, 209–218 (2008).
51. Kim, D. *et al*. SIRT1 deacetylase protects against neurodegeneration in models for Alzheimer's disease and amyotrophic lateral sclerosis. *EMBO J.* **26**, 3169–3179 (2007).
52. Dal-Pan, A., Pifferi, F., Marchal, J., Picq, J. L. & Aujard, F. Cognitive performances are selectively enhanced during chronic caloric restriction or resveratrol supplementation in a primate. *PLoS One* **6**, e16581 (2011).
53. Oomen, C. A. *et al*. Resveratrol preserves cerebrovascular density and cognitive function in aging mice. *Front. Aging. Neurosci.* **1**, 4 (2009).
54. Drapeau, E. *et al*. Spatial memory performances of aged rats in the water maze predict levels of hippocampalneurogenesis. *Proc. Natl. Acad. Sci. U. S. A.* **100**, 14385–14390 (2003).
55. Dupret, D. *et al*. Methylazoxymethanol acetate does not fully block cell genesis in the young and aged dentate gyrus. *Eur. J. Neurosci.* **3**, 778–83 22,778–783 (2005).
56. Drapeau, E., Montaron, M. F., Aguerre, S. & Abrous, D. N. Learning-induced survival of new neurons depends on the cognitive status of aged rats. *J. Neurosci.* **27**, 6037–6044 (2007).
57. Blau, C. W. *et al*. The age-related deficit in LTP is associated with changes in perfusion and blood-brain barrier permeability. *Neurobiol. Aging* **33**, 1005 e23–35 (2012).
58. Nikas, J. B. Inflammation and immune system activation in aging: a mathematical approach. *Sci. Rep.* **3**, 3254 (2013).
59. Liu, M. C. *et al*. Involvement of microglia activation in the lead induced long-term potentiation impairment. *PLoS One* **7**, e43924 (2012).
60. Kennedy, D. O. *et al*. Effects of resveratrol on cerebral blood flow variables and cognitive performance in humans: a double-blind, placebo-controlled, crossover investigation. *Am. J. Clin. Nutr.* **91**, 1590–1597 (2010).
61. Wong, R. H. *et al*. Acute resveratrol supplementation improves flow-mediated dilatation in overweight/obese individuals with mildly elevated blood pressure. *Nutr. Metab. Cardiovasc. Dis.* **21**, 851–856 (2011).
62. Ghanim, H. *et al*. An anti-inflammatory and reactive oxygen species suppressive effect of an extract of Polygonum cuspidatum containing resveratrol. *J. Clin. Endocrinol. Metab.* **95**, E1–E8 (2010).
63. Kohman, R. A. & Rhodes, J. S. Neurogenesis, inflammation and behavior. *Brain Behav. Immun.* **27**, 22–32 (2013).
64. Markowska, A. L. Sex dimorphisms in the rate of age-related decline in spatial memory: relevance to alterations in the estrous cycle. *J. Neurosci.* **19**, 8122–8133 (1999)
65. Burke, S. N. & Barnes, C. A. Neural plasticity in the aging brain. *Nat. Rev. Neurosci.* **7**, 30–40 (2006)
66. Price, N. L. SIRT1 is required for AMPK activation and the beneficial effects of resveratrol on mitochondrial function. *Cell Metab.* **15**, 675–690 (2012).
67. Hubbard, B. P. *et al*. Evidence for a common mechanism of SIRT1 regulation by allosteric activators. *Science* **339**, 1216–1219 (2013).
68. Shetty, G. A., Hattiangady, B. & Shetty, A. K. Oral treatment of resveratrol to aged rats enhances expression of pro-cognitive and anti-inflammatory genes in the hippocampus and eases cognitive dysfunction. *Society for Neurosci Abstracts* **608.05** (2013).
69. Dávila, D. & Torres-Aleman, I. Neuronal death by oxidative stress involves activation of FOXO3 through a two-arm pathway that activates stress kinases and attenuates insulin-like growth factor I signaling. *Mol. Biol. Cell.* **19**, 2014–2025 (2008).
70. Busch, F. *et al*. Resveratrol modulates interleukin-1β-induced phosphatidylinositol 3-kinase and nuclear factor kB signaling pathways in human tenocytes. *J. Biol. Chem.* **287**, 38050–38063 (2012).
71. Ren, Z. *et al*. Resveratrol inhibits NF-kB signaling through suppression of p65 and IkappaB kinase activities. *Pharmazie* **68**, 689–694 (2013).
72. Ge, J. F. *et al*. Antidepressant-like effect of resveratrol: involvement of antioxidant effect and peripheral regulation on HPA axis. *Pharmacol. Biochem. Behav.* **114–115**, 64–69 (2013).
73. Liu, D. *et al*. Resveratrol reverses the effects of chronic unpredictable mild stress on behavior, serum corticosterone levels and BDNF expression in rats. *Behav. Brain Res.* **264**, 9–16 (2014).
74. Park, H. R., Kong, K. H., Yu, B. P., Mattson, M. P. & Lee, J. Resveratrol inhibits the proliferation of neural progenitor cells and hippocampal neurogenesis. *J. Biol. Chem.* **287**, 42588–42560 (2012).
75. Hou, Y. *et al*. Mitochondrial superoxide production negatively regulates neural progenitor proliferation and cerebral cortical development. *Stem Cells* **30**, 2535–2547 (2012).
76. Morris, R. Development of a water-maze procedure for studying spatial learning in the rat. *Neurosci. Methods* **11**, 47–60 (1984).
77. Hattiangady, B., Kuruba, R. & Shetty, A. K. Acute seizures in old age lead to a greater loss of CA1 pyramidal neurons, an increased propensity for developing chronic TLE and a severe cognitive dysfunction. *Aging Dis.* **2**, 1–17 (2011).
78. Hattiangady, B. & Shetty, A. K. Neural stem cell grafting counteracts hippocampal injury-mediated impairments in mood, memory, and neurogenesis. *Stem Cells Transl. Med.* **1**, 696–708 (2012).
79. Andrus, B. M. *et al*. Gene expression patterns in the hippocampus and amygdala of endogenous depression and chronic stress models. *Mol. Psychiatry* **17**, 49–61 (2012).
80. Solberg, L. C. *et al*. Depressive-like behavior and stress reactivity are independent traits in a Wistar Kyoto × Fisher 344 cross. *Mol. Psychiatry* **8**, 423–433 (2003).
81. Parihar, V. K., Hattiangady, B., Shuai, B. & Shetty, A. K. Mood and memory deficits in a model of Gulf War illness are linked with reduced neurogenesis, partial neuron loss, and mild inflammation in the hippocampus. *Neuropsychopharmacology* **38**, 2348–2362 (2013).
82. Hattiangady, B. *et al*. Increased dentate neurogenesis after grafting of glial restricted progenitors or neural stem cells in the aging hippocampus. *Stem Cells* **25**, 2104–2117 (2007).
83. Shetty, A. K., Hattiangady, B., Rao, M. S. & Shuai, B. Deafferentation enhances neurogenesis in the young and middle-aged hippocampus but not in the aged hippocampus. *Hippocampus* **21**, 631–646 (2011).
84. Hattiangady, B., Rao, M. S. & Shetty, A. K. Plasticity of hippocampal stem/progenitor cells to enhance neurogenesis in response to kainate-induced injury is lost by middle age. *Aging Cell* **7**, 207–224 (2008).

Acknowledgments

This study was supported by grants from the National Institutes of Health (National Center for Complementary and Alternative Medicine R21 award, AT006256-03 to AKS), State of Texas (Emerging Technology Funds to AKS) and Department of Veterans Affairs (VA Merit Award to AKS).

Author contributions

M.K. and V.K.P. contributed equally to this work. M.K. performed statistical analyses of behavioral tests, stereological cell counts, immunohistochemistry, J imaging and Neurolucida tracing to quantify cognitive and mood function, hippocampus neurogenesis, microvasculature and microglia, prepared figure composites and the first version of the manuscript text. V.K.P. performed water maze and forced swim tests, administration of resveratrol, initial analyses of behavioral data and some experiments for neuronal differentiation of newly born cells. B.H. contributed to the experimental design, analyses and interpretation of behavioral data, analyses of neuronal differentiation of newly born cells using confocal microscopy, immunohistochemistry, photomicrography and preparation of composite figures. V.M. performed GFAP immunohistochemistry, J Imaging of astrocytes and the associated statistical analyses. B.S. performed animal perfusions, tissue processing, cryostat sectioning, histology, and BrdU and DCX immunohistochemistry. A.K.S. conceived the study, conceptualized the research design, interpreted all behavioral and immunohistochemical results and prepared the final version of manuscript text and figures. All authors gave input to the manuscript text and approved the final version of the manuscript.

Additional information

Supplementary information accompanies this paper at http://www.nature.com/scientificreports

Competing financial interests: The authors declare no competing financial interests.

How to cite this article: Kodali, M. *et al*. Resveratrol Prevents Age-Related Memory and Mood Dysfunction with Increased Hippocampal Neurogenesis and Microvasculature, and Reduced Glial Activation. *Sci. Rep.* **5**, 8075; DOI:10.1038/srep08075 (2015).